

Chapter 2

Fission Reactor Physics

Michael Natelson

Glossary

| | |
|---------------------------|--|
| Fissile | Fissile isotopes are fissionable by the capture of neutrons of any energy, but are especially easily fissioned by the capture of slow neutrons, for example, U^{233} , U^{235} , Pu^{239} , and Pu^{241} . |
| Fertile | Fertile isotopes may be transmuted into fissile isotopes by neutron capture. The naturally occurring fertile isotopes are Th^{232} and U^{238} . |
| Critical | A critical fission reactor is in a steady state, with its neutron population sustained by a chain reaction. |
| Reactivity | Reactivity is a dimensionless parameter, which characterizes how far from critical a fission reactor is. If zero, the reactor is critical; if positive, the reactor is supercritical and its neutron population is increasing; if negative, the reactor is subcritical. |
| Microscopic cross section | A microscopic cross section is a parameter, with dimensions of area, that is a measure of the probability of a particular reaction resulting from an incident particle on a target nucleus. The <i>macroscopic cross section</i> for this “particular” reaction is the microscopic cross section times the number density of the target nucleus. |

This chapter was originally published as part of the Encyclopedia of Sustainability Science and Technology edited by Robert A. Meyers. DOI:[10.1007/978-1-4419-0851-3](https://doi.org/10.1007/978-1-4419-0851-3)

M. Natelson (✉)

Retired from the Bettis Atomic Power Laboratory, West Mifflin, PA, USA

e-mail: MNatelson@aol.com

Definition of Subject

At the end of the nineteenth century and through the first half of the twentieth century, revolutionary discoveries were made in physics, and the laws of physics and our understanding of them were greatly expanded. In addition, tragic historical events led to an unprecedented concentration of intellectual talent and economic resources (the Manhattan Project) that allowed the new physics to be applied to the engineering of nuclear (fission) reactors. This entry will describe the advances in physics, which are key to fission reactor design, and how they enable this engineering practice.

Introduction

In 1900, Lord Kelvin (William Thomson) reportedly told the British Association for the Advancement of Science that “there is nothing new to be discovered in physics now. All that remains is more and more precise measurements.” Whether he actually said this or not, it is reasonable to believe that many scientists and engineers of his day would have concurred. Newton’s definitions and laws of mechanics and optics had long been successfully applied. Maxwell’s equations, Ohm’s law, etc. seemed to describe electricity and magnetism. Boltzmann and Gibbs had provided the foundations of statistical mechanics and thermodynamics. And chemists had been busy developing atomic theory, identifying 92 elements, the laws of chemical combination, the weights and sizes of atoms and molecules, and the periodic system.

With hindsight it is clear, however, that in 1900 there were many intriguing questions outstanding in the physical sciences, and there was an historically large cohort of scientists, being produced by the major universities of the day, ready to address them. The questions (and their resolutions) of prime importance to “fission reactor physics” are:

1. Does a theory of relativity apply to Maxwell’s equations, and is there a unique frame of reference (ether) for the propagation of light?
2. Why are the heaviest naturally occurring elements unstable, giving off various forms of “radiation” and transmuting to different elements?
3. What does the quantization of electromagnetic radiation (required to describe black body radiation energy spectra and the photoelectric effect) mean to the laws of physics on the atomic scale?

The resolution of each of these questions will be discussed in this entry, as they are the starting points for the accumulation of knowledge needed to characterize the workings of fission reactors.

Clearly, Einstein’s Theory of Relativity addressing question (1), and its identification of mass as a form of energy (1905) would, excuse the bad pun, energize

the whole effort. Already in 1914, H. G. Wells in his novel “The World Set Free” envisioned industrial atomic energy and atomic bombs used in a catastrophic world war.

At the end of the nineteenth century, electrochemists looking for heavy elements (heavier than lead and bismuth) found that “radiation” was given off by the materials they were investigating. Becquerel (1896) observed γ rays (penetrating electromagnetic radiation similar to x-rays) from uranium salts. The Curies (1898) observed α and β rays from polonium and radium. Rutherford showed that the positively charged α s were doubly ionized helium atoms. The β s are negatively charged electrons, the same particles as the cathode rays that Thomson characterized and named (1897). These “radiations” proved to be key tools for determining the structure of atoms. The α particle was shown by Rutherford (1911) and his coworkers to scatter from gold foil in a manner inconsistent with the atomic model of the day, Thomson’s *raisins (electrons) in the pudding* (positive charge medium) model. To explain the α scattering results, an atom’s positive charge and its mass, minus that of its electrons, needed to be concentrated in a small nucleus (radius $\sim 10^{-12}$ cm), with its electrons distributed over a much larger volume (radius $\sim 10^{-8}$ cm), that of the whole atom. Niels Bohr, inspired by Rutherford’s work, took to determining the *distribution* of atomic electrons. His success, building off Question (3) above, led to quantum mechanics. A complete model for the atom, however, still required an explanation for the mass of the nucleus. Again bombardment of various atoms (elements) with α particles led to the answer. Chadwick (1932) proved that the “rays” produced by α s striking beryllium nuclei were neutral particles with mass slightly greater than the hydrogen nucleus, the proton. These neutral particles are the neutrons that had been hypothesized by Rutherford 12 years earlier. Heisenberg (1932) produced a detailed model of the atomic nucleus where the mass number A is the total number of elementary particles, protons plus neutrons, making up a nucleus, and the nuclear charge is Z , the number of protons. Thus, there can be various *isotopes* for a given element, more than one A for a given Z .

The discovery of the neutron marked the start of furious activity, culminating in the operation of the first fission reactor only 10 years later. Leo Szilard in 1933 recognized that a neutral neutron with modest kinetic energy could penetrate an atomic nucleus and cause a reaction releasing nuclear (mass) energy, and if, as part of the “reaction,” additional neutrons were produced, a chain reaction could result. Szilard produced a patent for a reactor based on this idea and assigned it to the British Government in 1936 (before fission was discovered). In 1934, Fermi was using neutron bombardment (with neutrons of various energies) to produce nuclear transformations in many elements. Of special interest was the production of transuranic elements, Z greater than 92. Fermi won the 1938 Nobel Prize for this work. However, unknown at the time, he had also fissioned uranium. This was determined by electrochemical analysis of the products of neutron bombardment of uranium by Hahn and Strassmann. Subsequently, the process was identified as *fission* by Meitner and Frisch. Bohr recognized that the ease with which low energy neutrons could cause fission of uranium was due to the existence of the naturally occurring,

but low atom percent (0.72%), isotope ${}_{92}\text{U}^{235}$ [1] (Various notations have been used to designate a particular isotope, for example, for uranium with mass number (A) 235; ${}_{92}\text{U}^{235}$, U235, and ${}^{235}_{92}\text{U}$. The latter is in common use today. For ease of composition and for consistency with most of the references used in this entry the older standard, A as a right superscript, is used.). He and Wheeler, from their Theory of Fission [2], also recognized that the not yet produced isotope ${}_{94}\text{Pu}^{239}$, would also be readily fissioned by slow neutrons [3]. This was in early 1939. Bohr still did not think production of a fission bomb to be feasible.

Leo Szilard was, however, not deterred. He persuaded his friend Albert Einstein to write President Roosevelt (8/2/1939), urging government support of fission research and the stock piling of uranium. This ultimately led to the Manhattan Project. In 1940, Seaborg and McMillan synthesized the readily fissionable isotope of plutonium, ${}_{94}\text{Pu}^{239}$, which is produced by neutron capture in the dominant uranium isotope ${}_{92}\text{U}^{238}$. Wheeler credited Louis Turner [3] with pointing out that kilogram quantities of ${}_{94}\text{Pu}^{239}$ could be produced in a large fission chain reaction reactor. Fermi and Szilard [4] designed and built the prototype for such a reactor, a “pile” of graphite blocks containing an array of natural uranium pellets. It was constructed in a squash court under a grand stand of the University of Chicago’s Stagg Field, and went *critical* (sustained a chain reaction) on December 2, 1942. The Manhattan Project built large reactors of this type for weapons material production, and also successfully pursued means of enriching uranium in ${}_{92}\text{U}^{235}$. Enriched uranium allows more compact, higher power density, reactor designs.

The Manhattan Project brought together extraordinary scientific and engineering talent, and immense resources to produce the weapons that ended the Second World War. It also provided the foundation for all fission reactor development that has followed. The subsequent advances in “physics,” which have contributed to this development, are principally:

1. The full understanding of the interaction of neutrons with nuclei: scattering (elastic and inelastic), and capture (simple absorption, transmutation, and fission), including measuring the parameters that characterize the probabilities of these “interactions”
2. The formulation of methods to solve the neutron transport (Boltzmann) equation, which governs the behavior of the dilute “gas” of neutrons in a fission reactor

This entry will discuss the topics, pre- and post-Manhattan Project, which encompass the physics of fission reactors.

Mass–Energy Relationship

In his initial paper [5] on the theory of relativity, Einstein confronted the problem of guaranteeing that the laws of electromagnetism (Maxwell’s equations) apply in all inertial reference frames, just as the laws of mechanics do. In an inertial reference

frame, an object, which is at rest, remains at rest and an object traveling with a particular velocity will maintain that velocity. Einstein asserted that there is no preferred reference frame (like stationary *ether* in space, as postulated years earlier), and that the speed of light c , in vacuum, 2.998×10^8 m/s, is the same in all inertial reference frames. From these assertions, Einstein derived transformations for various variables in the laws of physics from one inertial reference frame to another. This solved the “electromagnetism” problem and provided a firm grounding (theory) for phenomena observed when velocities approach the speed of light. For examples of the latter, see Kaplan, “Nuclear Physics” on the charge-to-mass ratio of the electron as a function velocity, and Mermin, “It’s About Time,” on the half-life of unstable particles as a function of their velocity. Our interest here is specifically on the relationship between mass and energy resulting from the special (not applying to gravity) theory of relativity. What is meant by the ubiquitous formula.

$$E = Mc^2? \quad (2.1)$$

For application to fission, an inelastic collision between two particles will be treated for relativistic conditions. The approach presented by Mermin in “It’s About Time” will be used.

In an elastic collision, total momentum, $\mathbf{P} = \mathbf{p}_1 + \mathbf{p}_2$, mass, $M = m_1 + m_2$, and kinetic energy, $K = k_1 + k_2$ are all conserved, where the mass, m , is an inherent property of a particle and is a measure of how it resists a change in its velocity. In an inelastic collision, only total momentum, \mathbf{P} needs to be conserved. It needs to be conserved, however, in all inertial frames of reference. For relativistic conditions, one defines a particle’s momentum (a vector [in bold face]) as

$$\mathbf{p} = m\mathbf{u}/(1 - \mathbf{u}^2/c^2)^{1/2}, \quad (2.2)$$

where \mathbf{u} is the particle velocity. As is required for consistency between relativistic and nonrelativistic laws of mechanics, Eq. 2.2 is effectively the nonrelativistic definition of momentum for the particle speed, $u \ll c$. Now to find \mathbf{p}' , the particle momentum, in a frame moving with velocity \mathbf{v} relative to the frame in which the particle has velocity \mathbf{u} , one applies the relativistic translation law for velocities:

$$\mathbf{u}' = (\mathbf{u} - \mathbf{v})/(1 - \mathbf{u}\mathbf{v}/c^2). \quad (2.3)$$

Substituting for \mathbf{u}' in the expression for \mathbf{p}' (Eq. 2.2 with \mathbf{p} and \mathbf{u} primed), one obtains the relativistic translation law for momentum

$$\mathbf{p}' = (\mathbf{p} - p^0\mathbf{v})/(1 - \mathbf{v}^2/c^2)^{1/2}, \quad (2.4)$$

where

$$p^0 = m/(1 - \mathbf{u}^2/c^2)^{1/2}. \quad (2.5)$$

Now, if total momentum is to be conserved in our two-particle inelastic collision in both the primed and unprimed frames, then $P^0 = p_1^0 + p_2^0$ must also be conserved. Again, using the relativistic translation law for velocities (Eq. 2.3) and the definition p^0 (Eq. 2.5), we find that

$$p^{0'} = (p^0 - \mathbf{p}\mathbf{v}/c^2)/(1 - \mathbf{v}^2/c^2)^{1/2}. \quad (2.6)$$

And so for the *total* quantities we want to be conserved we have

$$\mathbf{P}' = (\mathbf{P} - P^0\mathbf{v})/(1 - \mathbf{v}^2/c^2)^{1/2} \quad \text{and} \quad (2.7)$$

$$P^{0'} = (P^0 - \mathbf{P}\mathbf{v}/c^2)/(1 - \mathbf{v}^2/c^2)^{1/2}. \quad (2.8)$$

Examining these expressions, it is clear that if \mathbf{P} and P^0 are not changed after an inelastic (or elastic) collision, then neither is \mathbf{P}' and $P^{0'}$.

In the limit of the speed u being much smaller than c , the difference between p^0 and m , $(p^0 - m)$, approaches $\mu^2/2c^2$. This result leads to a definition of relativistic kinetic energy, k , for a particle

$$k = p^0 c^2 - mc^2, \quad (2.9)$$

which has the required property of reducing to the nonrelativistic form, $\mu u^2/2$, in the limit of u much smaller than c .

Returning to our two-particle inelastic collision, as \mathbf{P} is conserved so is $P^0 c^2$ and thus from Eq. 2.9

$$\Delta M c^2 = \Delta K, \quad (2.10)$$

where ΔM is the change in the masses of the inputs and outputs of the collision participants, and ΔK is the change in the kinetic energies of these “inputs and outputs.” Thus, Eq. 2.10 provides insight into the meaning of “ $E = Mc^2$ ” for the fission process. For $n + {}_{92}\text{U}^{235} \mapsto \text{fission products} + 202.7 \text{ MeV}$ (the ΔK of Eq. 2.10 in unit of millions of electron volts) the percent change in mass can be estimated by dividing 202.7 MeV by the energy equivalents of the inputs (i.e., 236 amu, where 1 amu = 931.141 MeV). The result is $\sim 0.1\%$, which may not appear to be large until one makes a comparison with a chemical reaction. For example, $\text{O}_2 + \text{C} \rightarrow \text{CO}_2 + 4.1 \text{ eV}$. A similar calculation indicates a $1 \times 10^{-8}\%$ conversion of mass to kinetic energy. Since one could not measure such a small change in total input and output masses in chemical reactants, it is not surprising that the full impact of “ $E = Mc^2$ ” had to await demonstration in a nuclear reaction like fission. However, as will be discussed in the next three sections, the large energy release in fission, while conforming to Eq. 2.10, is due to the strength of the forces that hold a nucleus together and the charge repulsion forces that will accelerate two smaller nuclei as they are formed in the fissioning of a larger “parent” nucleus.

Heavy Elements

The “heavy elements” of particular importance to fission reactors are the radioactive nuclei, which are characterized by systematic chains of decay. In nature, there are three chains (series). In a given series, each nucleus has a *mass number*, A , governed by a simple formula with the variable the integer n (see [Table 2.1](#)), and is identified with its longest lived isotope, that is, Thorium, Uranium, and Actinium (U^{235} had not been discovered when the $4n + 3$ series was identified). These *longest half-lives* are not surprisingly comparable to the age of the earth, 4.5×10^9 years. Half-life is one of three related parameters of radioactive decay processes, $T_{1/2}$, λ , and τ . The fundamental equation of radioactive decay is

$$-dN(t)/dt = \lambda N(t), \quad (2.11)$$

where λ is the *decay constant*, and $N(t)$ is the number of decaying nuclei at time t . The solution of [Eq. 2.11](#) is

$$N(t) = N(0)e^{-\lambda t}. \quad (2.12)$$

The time when an original inventory of decaying nuclei, $N(0)$, is halved is

$$T_{1/2} = \ln 2 / \lambda = 0.693 / \lambda. \quad (2.13)$$

And as the decay process is statistical the *mean life-time*, τ , of a decaying nucleus is

$$\tau = (1/N(0)) \int_0^{\infty} N(0)\lambda t e^{-\lambda t} dt = 1/\lambda, \quad (2.14)$$

the reciprocal of the decay constant.

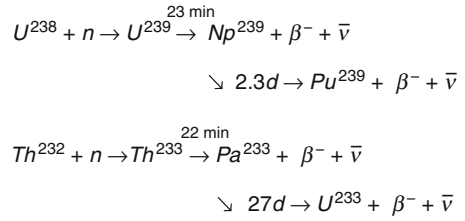
With the search for transuranic elements through the bombardment of the heaviest natural elements, primarily with neutrons, a fourth decay series was identified, the Neptunium ($A = 4n + 1$) series whose radioactive members are not found in *nature* (see [Table 2.1](#)).

Table 2.1 Heavy element decay series

| Series name | Type | Final stable nucleus | Longest lived nucleus | Longest half-life (years) |
|---------------------------------|----------|----------------------|-----------------------|---------------------------|
| Thorium | $4n^a$ | Pb^{208} | Th^{232} | 1.41×10^{10} |
| Uranium | $4n + 2$ | Pb^{206} | U^{238} | 4.47×10^9 |
| Actinium | $4n + 3$ | Pb^{207} | U^{235} | 7.04×10^8 |
| Neptunium, not in <i>nature</i> | $4n + 1$ | Bi^{209} | Np^{237} | 2.14×10^6 |

^a n is an integer

Fig. 2.1 Transmutation of fertile to fissile nuclei. ($\bar{\nu}$ is the antineutrino, the chargeless, \sim zero mass particle that accompanies β emission)



Of the “heavy elements,” the isotope U^{235} is key to fission reactor design. It is the only naturally occurring isotope which readily fissions when bombarded with neutrons of all energies. While its atomic percent abundance, 0.72%, is small, it is large enough to support chain reactions in reactors where neutrons born in fission are slowed down (moderated) by graphite (carbon) or by heavy water (deuterium oxide). When Uranium is enriched in U^{235} ($\sim 3\text{--}5\%$), it can fuel reactor designs where ordinary water moderates fission neutrons (today’s pressurized water and boiling water reactors). Having U^{235} available as a reactor fuel makes it possible to exploit the two abundant *fertile* “heavy elements,” U^{238} and Th^{232} . The term “fertile” refers to the fact that when these elements absorb a neutron they can be transmuted to *fissile* isotopes (Pu^{239} and U^{233} respectively), which like U^{235} readily fission when bombarded by neutrons of all energies. The transmutation processes are shown in Fig. 2.1. It is important to note that only one neutron capture is required in each of these transmutations. In a reactor design, neutron economy is the key to maintain a chain reaction and, as will be discussed in the section on [Future Directions](#), expending one neutron with a reasonable probability of obtaining an additional fissile nucleus is a winner.

The heavy element radioactive decay series are also important to safety in fission reactor design. Each of the decay processes, α and β^- emissions and associated γ s, is favorable to energy release. So any heavy elements, particularly transuranics, in a reactor’s fuel system will contribute to the *decay heat* load that must be dissipated when a reactor shuts down. As will be discussed in the next section, the major short-term contributors to decay heat are *fission products*. A power reactor that shuts down following a sustained run at full rating will initially produce $\sim 7\%$ of that rating from decay heat, even if the chain reaction and nearly all fissioning has ceased.

For a full discussion of the radioactive decay series and the particulars of α , β^- , β^+ and γ emission, see Kaplan, and Krane, “Introductory Nuclear Physics.”

Fission and Its Products

As noted in the [Introduction](#), fission was discovered accidentally during the search for transuranic elements. This work by Fermi and others was part of an extensive effort to understand the atomic nucleus and to duplicate the great success of quantum mechanics and the Pauli exclusion principle in providing a fully

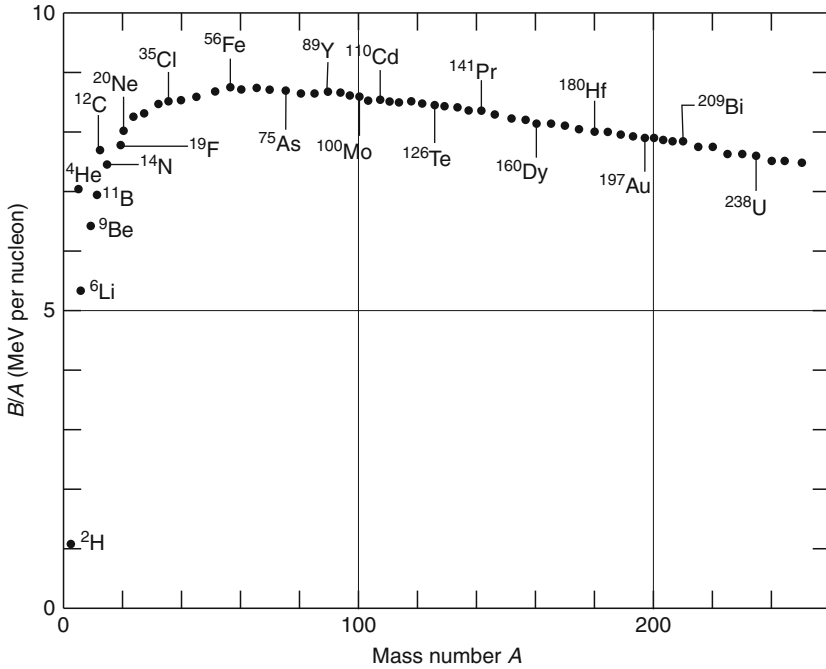


Fig. 2.2 Binding energy per nucleon (Krane)

predictive *Theory* of atomic electron structure. A comparable theory for the nucleus has not been developed, but several models (e.g., shell and liquid drop) provide insight into the trends and correlations found in the data provided by the extensive experimentation performed on the nuclei of the various elements and their isotopes.

Measurements of atomic mass ($m(X^A)$), and the mass of the electron, proton, and neutron, yields the *binding energy*, B , of a nucleus, ${}_Z X^A$, the work (energy) required to disassemble a nucleus into its neutrons and protons:

$$B = \{Zm_p + Nm_n - (m(X^A) - Zm_e)\}c^2, \quad (2.15)$$

where Z is the atomic number (the number of protons) and $N = A - Z$ is the number on neutrons. (The binding energy of atomic electrons is ignored as negligible compared to the other factors in Eq. 2.15.)

Plotting the ratio of measured binding energies B to corresponding mass number A (Fig. 2.2) immediately makes evident the potential of energy release from fission of heavy element. Note the B/A versus A “curve” has a flat maximum in the middling A range $\sim 50 \rightarrow \sim 150$, and falls off (decreases) as A increases. Thus, there is a potential energy excess if a heavy element (isotope) can be disassembled and reassembled as two mid-range isotopes (preserving total A , Z , and N). (The behavior of the B/A curve for light elements shows the potential energy release from fusion.) Obviously fission (nor fusion) does not take occur “naturally” on earth

today (There is convincing evidence that a naturally occurring chain reaction took place in a uranium deposit in Gabon about 2×10^9 years ago, when the abundance of U^{235} would have been $\sim 3\%$, high enough for a water-moderated “reactor” to operate. The higher earlier abundance is due to the shorter half-life of U^{235} (7.0×10^8 y) relative to that of U^{238} (4.4×10^9 y). See Krane for an excellent discussion of the Gabon reactor). The remainder of this section is devoted to particular requirements for fission to take place and to the discussion of the resulting fission products and their energies.

Insights provided by examining binding energies, and by additional experiments to determine nucleon–nucleon forces have led to the Shell and Liquid Drop models of the nucleus. Features of these models are incorporated in the *semiempirical mass formula* (Eq. 2.16). While a thorough discussion of the nuclear models is beyond the scope of this entry (see Kaplan or Krane), the mass formula provides key information on fission, energy release, and the relative likelihood for various nuclei.

In the semiempirical mass formula, the binding energy has five terms, which will be discussed below.

$$m({}_Z X^A) = Zm_p + Nm_n - [B_0 + B_1 + B_2 + B_3 + B_4]/c^2. \quad (2.16)$$

$B_0 = a_v A$ is the volume energy. Note in Fig. 2.2 that B/A saturates, thus B_0 has a linear dependence on A . The attractive nuclear forces between nucleons (n–n, n–p and p–p) are all equal and short range, smaller than the radius of the nucleus, $r = r_0 A^{1/3}$ where $r_0 \sim 1.2 \times 10^{-12}$ cm. If the range were larger, there would be attraction between each nucleon pair and B_0 would depend on $A(A - 1)$.

$B_1 = -a_s A^{2/3}$, is the negative surface decrement. As the nucleon–nucleon forces are “short range,” neutrons and protons on the surface of a nucleus are less tightly bound.

$B_2 = -a_c Z(Z-1)/A^{1/3}$, is the coulomb repulsion decrement. While the nuclear forces are strong enough to overcome coulomb forces, the protons in the nucleus do repel and reduce binding energy. Assuming a uniform distribution of protons in a liquid drop model of a spherical nucleus, an electrostatics calculation yields the dependence of B_2 the number of proton pair, $Z(Z-1)$, and a measure of their spacing, $A^{1/3}$.

$B_3 = -a_a |N-Z||N-Z|/A$, is the neutron–proton population asymmetry decrement. As nuclei become heavier, more neutrons than protons are needed to overcome coulomb repulsion. However, as the shell model of the nucleus demonstrates when nucleons, neutrons and/or protons, are added to form heavier elements and their isotopes, they fill *shells* of successively higher energy and are thus less tightly bound. This is analogous to the case of atomic electrons. Neutrons and protons have half-integral spin like the electrons, and therefore no two neutrons (or protons) can occupy the same state in a nucleus in conformance with the Pauli exclusion principle. So B_3 is negative and proportional to the neutron excess and the fraction of the nucleus the excess represents.

Table 2.2 Heavy nuclei fission

| Target nucleus | Compound nucleus | E_e , Excitation energy (MeV) | E_a , Activation energy (MeV) |
|----------------|------------------|---------------------------------|---------------------------------|
| U^{233} | $[U^{234}]$ | 6.6 | 4.6 |
| U^{235} | $[U^{236}]$ | 6.4 | 5.3 |
| Pu^{239} | $[Pu^{240}]$ | 6.4 | 4.0 |
| U^{238} | $[U^{239}]$ | 4.9 | 5.5 |
| Th^{232} | $[Th^{233}]$ | 5.1 | 6.5 |

$B_4 = +\delta A^{-3/4}$ for even Z even N nuclei, $= 0$ for odd A nuclei, $= -\delta A^{-3/4}$ for odd Z odd N nuclei, is the pairing energy. As nucleons are added and fill *shells*, they are more tightly bound as spin up and spin down pairs. B_4 is important in determining the relative binding of isotopes of a given element and their propensity to fission.

A set of parameters for B which best fit the B/A curve (Fig. 2.2) is provided by Krane; $a_v = 15.5$ MeV, $a_s = 16.8$ MeV, $a_c = 0.72$ MeV, $a_a = 23$ MeV, and $\delta = 34$ MeV.

The potential for, and magnitude of, energy release from fission, whether as spontaneous decay or induced by particle or gamma ray capture, can be assessed with the semiempirical mass formula. As for an estimate of the magnitude of energy release, the B/A curve, as noted earlier, can be used directly. For example, the B/A for U^{238} is ~ 7.6 MeV. If it fissioned into two approximately equal mass nuclei ($A = 119$), their B/A would be ~ 8.5 MeV when in a ground state, and being more tightly bound than their parent (U^{238}) 214 MeV ($= 2 \times 119 \times 8.5 - 238 \times 7.6$) will be available through conservation of energy as kinetic energy of the daughter nuclei and of other fission products (neutrons, β s, γ s, and neutrinos). That this energy is *available* does not mean that there is a significant probability that fission occurs. In this example, which represents spontaneous fission of U^{238} , one finds in nature that this mode of U^{238} decay competes poorly with α decay (Spontaneous fission is a significant mode of decay for some transuranic isotopes found in depleted reactor fuel, particularly Pu^{240} and Pu^{241}). For fission fragments, daughter nuclei, to separate in spontaneous or induced fission, a potential barrier must be overcome. The height of the barrier relative to the ground state of a fission parent nucleus is called the *fission activation energy* (E_a). It can be estimated with the liquid drop model by calculating the change in the parent nucleus binding energy (B_1 and B_2) between the ground-state spherical configuration and a volume-conserving dumb-bell configuration (ref. [2] and [6]). Table 2.2 contains values of E_a for the *compound* nuclei formed by neutron capture in the fissile and fertile isotopes of primary interest in reactor design. These are compared with the *excitation energy* (E_e) provided in forming the compound nucleus.

$$E_e = [(m({}_Z X^A) + m_n) - m({}_Z X^{A+1})]c^2. \quad (2.17)$$

Note that E_e does not include any kinetic energy contribution from the captured neutron. For the fertile target nuclei (U^{238} and Th^{232}), $E_e < E_a$ and neutron kinetic energy will be required to overcome or quantum mechanically penetrate (with high

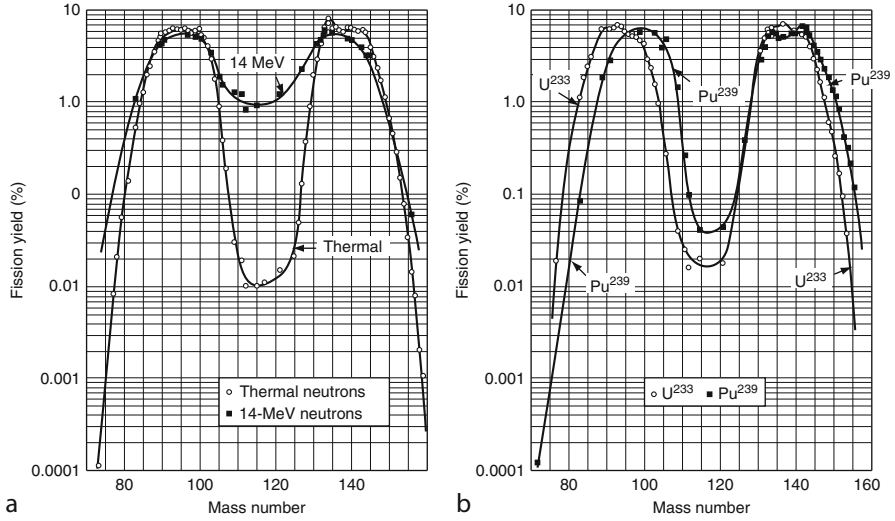


Fig. 2.3 Fission yields: (a) for U^{235} from fast and thermal neutrons, (b) for U^{233} and Pu^{239} from thermal neutrons [33]

probability) the potential barrier to fission. For the fissile targets, $E_c > E_a$ and thus “slow” neutrons can initiate fission.

The high values of E_c for the fissile targets are due to the positive “pairing” contribution, B_4 , to the binding energy of the compound nucleus ground states. Note $_{92}\text{U}^{234}$, $_{92}\text{U}^{236}$, and $_{94}\text{Pu}^{240}$ are all even Z even N nuclei and the corresponding target nuclei are even Z odd N . So, the second term in Eq. 2.17 is decreased by $\delta(A+1)^{-3/4}$, and B_4 is zero in the first term. Thus, an increase in E_c relative to the result if pairing is ignored is achieved. For fertile targets (even Z even N), roles are reversed. It is the first term in Eq. 2.17 that is decreased and B_4 is zero in the last term. Thus, E_c is lower than if pairing is ignored.

The semiempirical mass formula and the shell and liquid drop models are limited in predicting the fission process. This is best illustrated by the mass distribution of the major fission fragments (see Fig. 2.3). In the vast majority of cases, fission yields two unstable (having excess neutrons) nuclei, but not of equal mass, as in the example above used to estimate the energy available from spontaneous fission of U^{238} . The two humped curves in Fig. 2.3 are not predicted by nuclear models. To quote Krane, “surprisingly, a convincing explanation for this mass distribution has not been found.”

From the nuclear models, it is not surprising that free (prompt) neutrons are emitted in fission as the daughter nuclei are so rich in neutrons, but the prediction of their number (~ 2.5 on average) and energy spectrum (the mean ~ 2 MeV, see Fig. 2.4) are still an active area of study. The decay chains of the neutron-rich, excited daughter nuclei (fission fragments) are well predicted, including the release of (delayed) neutrons when in some cases neutron decay competes

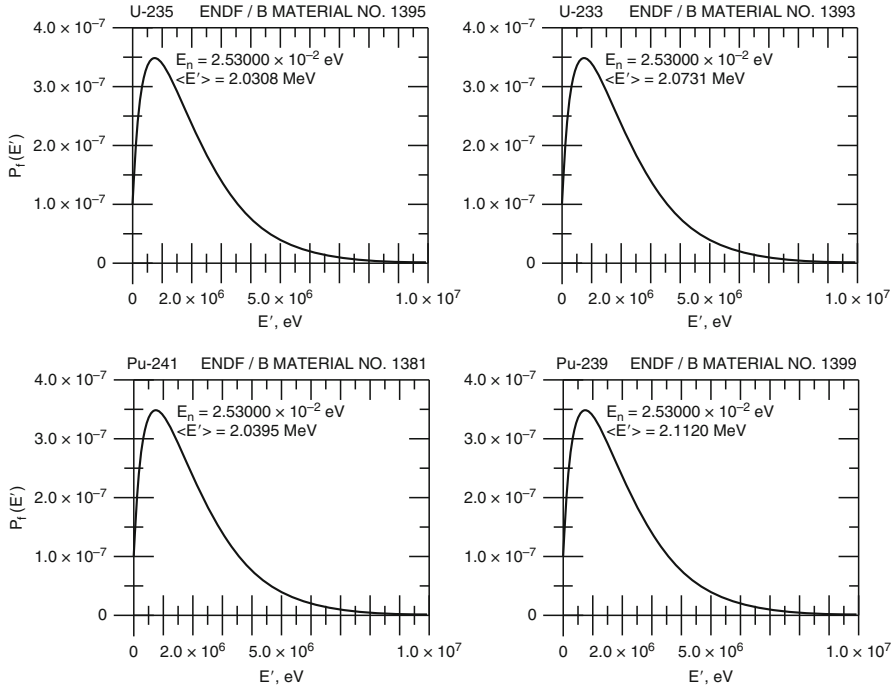


Fig. 2.4 Prompt neutron energy spectra where $P_f(E')$ is the probability per unit energy [32]

successfully with β -decay. The delayed neutrons are a small fraction of the total neutron emission (0.64% for thermal fission of U^{235}), but as will be discussed in section “[Fission Reactor Performance](#)”, they are important to reactor control.

Total energy release from the various neutron-induced fissions of interest in reactor design is remarkably consistent with the simple spontaneous U^{238} fission calculation made above. Of course, the constituents are different, as displayed in [Table 2.3](#).

In a reactor design, the total energy values in [Table 2.3](#) are not used. First, the contribution from neutrinos is subtracted, as their range before collision is well beyond reactor boundaries. Then, the energy release per fission from neutron captures which produce β s and γ s is added. The magnitude of this release is design-dependent as it is a function of the materials used, and the neutron capture rate in these materials. For plant energy balance studies, using 200 MeV/fission is satisfactory.

The problem of *decay heat* was noted in the previous section. From [Table 2.3](#), it can be seen that fission product decay is the immediate concern when a chain reaction is terminated. Assume full power from U^{235} fissioning, when this ceases, delayed γ s and β s are still being released. Thus, $\sim 6.3\%$ ($\simeq 100 \times (6.26 + 6.43)/200$) of rated power, coming from fission product decay, must still be dissipated, along with energy from the decay of transuranic elements present in the reactor, for a total of $\sim 7\%$.

Table 2.3 Energy yield in MeV from fission. Thermal neutron fission of fissile isotopes; fertile isotope fission is from neutrons with energy spectrum of a light water-moderated reactor [7, 32]

| Energy | Fissile or fertile isotope [†] | | | | | |
|---------------------------------|---|------------------|------------------|------------------|-------------------|-------------------|
| | ²³³ Th | ²³⁸ U | ²³⁵ U | ²³³ U | ²³⁹ Pu | ²⁴¹ Pu |
| Fission fragment kinetic energy | 162.1 ± 1.5 | 170.0 ± 0.66 | 169.6 ± 0.7 | 168.7 ± 0.7 | 175.9 ± 0.1 | 175.5 ± 1.1 |
| Prompt neutron kinetic energy | 4.7 ± 0.12 | 5.51 ± 0.1 | 4.79 ± 0.07 | 4.9 ± 0.1 | 5.9 ± 0.1 | 5.99 ± 0.13 |
| Delayed neutron kinetic energy | 0.024 ± 0.004 | 0.021 ± 0.003 | 0.0071 ± 0.0007 | 0.0014 ± 0.0005 | 0.001 ± 0.0005 | 0.0074 ± 0.0015 |
| Prompt γ rays | 6.15 ± 1.75 | 6.28 ± 0.8 | 6.96 ± 0.7 | 7.59 ± 0.71 | 7.74 ± 0.45 | 7.86 ± 1.8 |
| Delayed γ rays | 8.01 ± 0.2 | 8.04 ± 0.08 | 6.26 ± 0.05 | 4.99 ± 0.04 | 5.16 ± 0.1 | 6.33 ± 0.07 |
| β particles | 8.28 ± 0.21 | 8.25 ± 0.08 | 6.43 ± 0.05 | 5.13 ± 0.04 | 5.3 ± 0.1 | 6.51 ± 0.04 |
| Neutrino energy | 11.1 ± 0.3 | 11.14 ± 0.11 | 8.68 ± 0.06 | 6.91 ± 0.05 | 7.15 ± 0.11 | 8.78 ± 0.09 |
| Total energy yield | 200.3 ± 0.5 | 209.3 ± 0.3 | 202.7 ± 0.1 | 198.2 ± 0.1 | 207.2 ± 0.3 | 211.0 ± 0.3 |

Over 800 fission fragment nuclei have been identified. Their decay must be tracked to account for *decay heat* in reactor shut-down safety analysis and for the proper handling and storage of spent fuel (where both energy release and the nature of radiation fields must be known). One hundred and two of these nuclei are delayed neutron precursors. To simplify reactor transient (kinetics) calculations, the precursors are collected into six *effective* groups, where members of a given group have similar decay constants (see Table 2.4).

The energy spectra for a given delayed group do not vary significantly with fissioning isotope. The spectra are much softer (with lower mean energies, < 1 MeV) than for prompt neutrons [7]. This means that a delayed neutron in a thermal reactor is more *important* than a prompt neutron. It is more likely to reach the low energies (< 0.625 eV) where most fission occurs. Delayed neutrons can also result from other reactions, for example, photon capture (γ, n) (The expression (a,b) is shorthand for a nuclear reaction with an input particle “a” and output particle “b”, where the target and product nuclei are understood.) and neutron activation (n,p) followed by neutron decay of the product nucleus. If important to a particular reactor design, these delayed neutrons can be included by modifying the effective delayed group structure.

The final aspect of the ~ 800 fission fragment nuclei that must be dealt with is their impact on neutron balance. Each of them has a probability of capturing neutrons and in some case of causing a transmutation into a nucleus with a particularly large propensity for capturing neutrons. The nuclei of greatest importance to neutron balance are listed in Table 2.5.

I^{135} is important as it is the direct precursor of Xe^{135} , an especially large absorber of thermal neutrons. The next two isotopes in the table are precursors to a decay chain with three large absorbers, Pm^{147} , Sm^{149} , and Sm^{151} . The final five, with their precursors in parentheses, are large absorbers, but not as sensitive to neutron energy spectrum and power level and history as the others. Clearly, data for the 800 fission fragments must be handled through large computer files [8]. For neutron balance, the fission fragment isotopes, which are not treated explicitly (Table 2.5), can be lumped into an effective fission product nucleus with a yield per fission and *probability* for neutron capture. How one characterizes the *probability* of nuclear reactions is the subject of the next section.

Cross Sections

The nuclear reactions of importance to fission reactor design are by *definition* governed by the postulates of quantum mechanics (i.e., they are on the dimensional scale of the nucleus). And, thus the results of the various reactions are probabilistic in nature. The probability of a particular result is characterized by a parameter, the *microscopic* cross section, σ , with, not surprisingly, the dimensions of area, and which is quoted in units of *barns*. The barn, 10^{-24} cm², is a reasonable measure as in some cases σ is nearly the projected

Table 2.5 Direct yield fractions ($\times 100$) for isotopes in the most important fission product chains [32]

| Fission Product | Fissile or fertile isotope ^a | | | | |
|--|---|------------------|------------------|------------------|------------------|
| | ²³² Th | ²³⁸ U | ²³⁵ U | ²³³ U | ²³⁹ U |
| ¹³⁵ I | 5.238 | 6.548 | 6.349 | 4.860 | 6.303 |
| ¹³⁵ Xe | 0.0403 | 0.0150 | 0.255 | 1.337 | 1.152 |
| ¹⁴⁷ Nd | 3.08 | 2.711 | 2.271 | 1.775 | 2.073 |
| ¹⁴⁹ Pm | 0.825 | 1.765 | 1.089 | 0.769 | 1.261 |
| ⁹⁹ Mo (⁹⁹ Tc) | 2.965 | 6.247 | 6.127 | 4.957 | 6.144 |
| ¹⁰³ Ru (¹⁰³ Rh) | 0.164 | 6.336 | 3.137 | 1.707 | 6.991 |
| ¹³¹ I (¹³¹ Xe) | 1.481 | 2.982 | 2.473 | 2.352 | 3.093 |
| ¹³³ I (¹³³ Cs) | 3.858 | 6.356 | 6.787 | 5.974 | 6.923 |
| ¹⁴³ Ce (¹⁴³ Nd) | 6.619 | 4.834 | 5.972 | 5.881 | 4.561 |

^aThe energy of the neutron initiating the fission is in the thermal range for ²³⁵U, ²³³U, and ²³⁹Pu. For ²³²Th and ²³⁸U, the yields are due to fissions initiated by neutrons with a spectrum of energies typical of light water-moderated nuclear reactors.

area of a target nucleus, $4\pi R^2$, and R is $\sim 10^{-12}$ cm. Thus, envisioning a target foil of area, A , and thickness, dx (where dx is small enough to have negligible shadowing of one nucleus by another in the target foil), the probability that an incident particle in traveling a short distance (i.e., dx) will undergo a specific reaction equals $\sigma \rho A dx / A$, where ρ is the density of target nuclei ($\#/\text{cm}^3$) in the foil. It follows that to find the reaction rate in the foil we need the number of impinging particles per second. Given the particles have a density N ($\#/\text{cm}^3$) and are monoenergetic and monodirectional (normal to the face of the foil) with speed v , the number impinging per second equals $N \cdot (v dt) \cdot A / dt$. So the total reaction rate in the foil is $(NvA)(\rho \sigma dx)$, and the rate per cm^3 is $vN\rho\sigma$. The parameters that make up this specific rate have been reordered to reflect conventional definitions in reactor physics (In the nuclear engineering discipline, *reactor physics* refers to the portion of the field addressed in this entry):

$$vN \equiv \Psi_{\text{particle flux}}, \text{ and} \quad (2.18)$$

$$\rho\sigma \equiv \Sigma_{\text{macroscopic cross section}}. \quad (2.19)$$

The *flux* in our simple foil example is the number of particles per cm^2 per second crossing a plan parallel to the face of the foil. Given the more general representation of particle density (which will be used in the next section):

$N(\mathbf{r}, E, \mathbf{\Omega}, t) d\mathbf{r}^3 dE d\mathbf{\Omega} \equiv$ no. of particles in $d\mathbf{r}^3$ about \mathbf{r} , with kinetic energies in dE about E , and going in the solid angle $d\mathbf{\Omega}$ about the unit direction vector $\mathbf{\Omega}$ (see Fig. 2.5), at time t ; then the corresponding definition of *flux*, $\Psi(\mathbf{r}, E, \mathbf{\Omega}, t) ds dE d\mathbf{\Omega}$, is the no. of particles with E in dE going in direction $\mathbf{\Omega}$ in $d\mathbf{\Omega}$ that pass through the surface ds , which is located at \mathbf{r} and is normal to $\mathbf{\Omega}$, per unit time, at time t .

The *macroscopic* cross section is the probability that a particle undergoes a reaction characterized by σ , per unit path (for small paths, dx) traversed by the particle in a homogenous material with target nucleus density, ρ . This definition

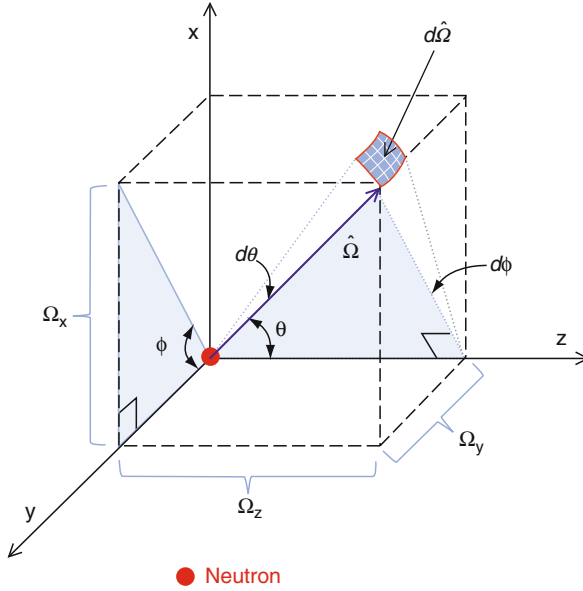


Fig. 2.5 The unit direction vector $\hat{\Omega}$ associated with neutron velocity and the differential (small) solid angle $d\hat{\Omega}$ which defines the range of directions

lends a special significance to $1/\Sigma_T$, where $\Sigma_T = \rho\sigma_T$. σ_T is the *total* microscopic cross section, the sum of the σ s for all of the reactions that the initiating particle can undergo with a given target isotope. So the change in flux, where $\hat{\Omega}$ is parallel to the x axis of a target material sample, over a small interval dx in the sample is $d\Psi = -\Psi\Sigma_T dx$. And thus, $\Psi(x) = \Psi(0) e^{-\Sigma_T x}$, where x is the distance into the “sample” (which has its face in the $y-z$ plane at $x=0$). So, the probability of a reaction in dx about x can be expressed as

$$P(x)dx = \Sigma_T dx \bullet (\Psi(x)/\Psi(0)) = \Sigma_T e^{-\Sigma_T x} dx. \quad (2.20)$$

And thus the *mean free path* of a particle in an incident beam ($\Psi(0)$) before being removed from the beam in a homogeneous target is

$$\bar{x} = \int_0^{\infty} dx x P(x) = 1/\Sigma_T. \quad (2.21)$$

or generally the *mean free path* is the average distance traveled between successive interactions.

If a homogeneous material is made up of various nuclei (elements/isotopes, indexed by j), then the macroscopic cross section for a reaction, i , is

$$\Sigma_i = \sum_j \rho_j \bullet \sigma_i^j. \quad (2.22)$$

The reactions of primary interest in fission reactor design are those initiated by neutrons and gammas. Neutron cross sections are key to determining if a chain reaction can be maintained, and that the neutron population can be controlled under various transient conditions (e.g., start-ups and shutdowns, planned and accidental), and, of course, the fission distribution in the reactor. Most of the resulting energy release, from fission fragments, is deposited locally in the fuel elements of a given design. However, gammas, from fission and neutron capture in reactor structures, have large mean free paths, and their distribution and capture rates must be determined, using gamma cross sections, to complete the knowledge of energy deposition. The subsequent engineering problem is to assure that the reactor cooling system can remove the deposited energy under normal and accident conditions. Neutron and gamma cross sections are also required for the shield design of a fission reactor.

Neutron reactions are characterized by their energy balance, the Q factor, as well as microscopic cross sections. For the simple reaction (with the target at rest),



the energy balance is

$$(E_n + m_n c^2) + M_X c^2 = (E_Y + M_Y c^2) + (E_y + m_y c^2), \quad (2.24)$$

and Q is defined as the difference in the kinetic energies of the inputs (here the neutron) and the outputs:

$$Q = E_Y + E_y - E_n \text{ or } = (M_X + m_n - M_Y - m_y)c^2. \quad (2.25)$$

If Q is positive, the reaction is exothermic, if negative, endothermic. For an endothermic reaction to go, for the microscopic cross section to be nonzero, enough kinetic energy must be supplied by the neutron to excite a compound nucleus, X^{A+1} , so it will decay to $Y + y$. As momentum must be conserved,

$$m_n v_n = (M_X + m_n) V_c \text{ or } V_c = v_n m_n / (M_X + m_n), \quad (2.26)$$

where V_c is the velocity of the compound nucleus. Then, the neutron energy supplied must be such that

$$-Q = m_n v_n^2 / 2 - (M_X + m_n) V_c^2 / 2 \quad (2.27)$$

and the *threshold energy*, E_{th} , for the reaction is

$$E_{th} = m_n v_n^2 / 2 = (-Q)(1 + m_n / M_X). \quad (2.28)$$

(n , $2n$) is an example of an endothermic reaction whose cross sections will exhibit an energy dependence of zero until the neutron energy E reaches an E_{th} .

The simplest, but very important, neutron reaction to be considered is a form of elastic scattering ($Q = 0$), where collisions can be treated with classical mechanics as hard sphere, billiard ball, interactions. For the energies of neutrons in fission reactors, 0–10 MeV, elastic scattering cross sections for most nuclei are constant and proportional to the square of the nuclear radius, $\sim A^{2/3}$. Assuming the target nucleus to be at rest and applying conservation of energy and momentum in the center of mass, CM, coordinate system, one determines the probability that the final energy of the scattered neutron, in the laboratory coordinate, LM, system, is E_f in dE_f :

$$\begin{aligned} P(E_i \rightarrow E_f) &= 1/(1 - \alpha)E_i, \text{ for } \alpha E_i \leq E_f \leq E_i \\ &= 0 \text{ otherwise,} \end{aligned} \quad (2.29)$$

where $\alpha = ((A-1)/(A+1))^2$ and E_i is the initial neutron energy. A is the mass number of the target nucleus. And, scattering is assumed to be isotropic in the CM coordinate system. This is a good assumption for the energy range of interest here, and its basis will be discussed later in this section. A full derivation of Eq. 2.29 can be found in Duderstadt and Hamilton, “Nuclear Reactor Analysis.” Examining $P(E_i \rightarrow E_f)$ one sees that a neutron scattering off a hydrogen nucleus ($A = 1$) can lose all its energy (as $\alpha = 0$). On average, it loses half its initial energy as

$$\bar{E}_f = \int_{\alpha E_i}^{E_i} dE_f E_f P(E_i \rightarrow E_f) = E_i(1 + \alpha)/2, \text{ and} \quad (2.30)$$

$$\Delta \bar{E} = E_i \rightarrow \bar{E}_f = E_i(1 - \alpha)/2. \quad (2.31)$$

Given $P(E_i \rightarrow E_f)$ as in Eq. 2.29, one defines *differential* microscopic elastic scattering cross sections, $\sigma_{es}^j(E_i)P(E_i \rightarrow E_f)dE_f$, which are particularly useful in determining how neutrons, born in fission, are slowed down in reactors designed to take advantage of the large fission cross sections of fissile isotopes in what is conventionally defined as the *thermal* neutron energy range, less than 0.625 eV. The superscript “j” of σ_{es}^j refers to the nuclei of the various *moderators* (hydrogen, deuterium and carbon) that are employed in these thermal reactors.

Once neutrons have slowed to the thermal range the target nuclei can no longer be assumed to be at rest. The interaction frequency will then be

$$|\mathbf{v} - \mathbf{V}| \sigma(|\mathbf{v} - \mathbf{V}|)\rho, \quad (2.32)$$

where $|\mathbf{v} - \mathbf{V}|$ is the relative speed of neutron and target. For elastic scattering, $\sigma(|\mathbf{v} - \mathbf{V}|)$ is still nearly constant and an *average* cross section for *thermal* neutrons with speed v ($= (2E/m_n)^{1/2}$) is

$$\bar{\sigma}(v) = (\sigma_{es}/v\rho) \int d^3V |\mathbf{v} - \mathbf{V}| \rho(\mathbf{V}), \quad (2.33)$$

where for many reactor applications the Maxwell–Boltzmann velocity distribution for ideal gases in thermal equilibrium at absolute temperature, T , can be used to represent the targets. Thus,

$$\rho(\mathbf{V}) = \rho \bullet (M/(2\pi kT))^{3/2} \exp(-MV^2/2kT), \quad (2.34)$$

where M is the mass of the target nucleus and k is the Boltzmann constant (8.6174×10^{-5} eV/K, K is degrees Kelvin).

From Eq. 2.33, one sees that for $v \gg V$ the *average* cross section is, as expected, σ_{es} . And, as the neutron speed decreases and approaches zero, the *average* cross section goes as one over the neutron speed.

For highly accurate calculations (As part of the process of evaluating nuclear data sets, very accurate calculations of integral experiments are made. Zero power *mockups* of reactors, with carefully recorded dimensions and inventories, are commonly used. Monte Carlo calculations (to be discussed in the next section) of neutron balance in the mockups are made with various data sets (e.g., cross-section libraries) to determine a recommended set. See the CESWG web site for references to such experiments.), more sophisticated treatments of scattering from moderator structures (e.g., molecules in liquids, lattices for solids) are required. The excitation of modes of vibration, and thus energy loss to phonons must be considered. This has been a fertile field of development [9] and double differential scattering cross sections for various moderators have been produced. They are of the form:

$$\begin{aligned} \sigma_s(E_i \rightarrow E_f, \Omega_i \rightarrow \Omega_f) dE_f d\Omega_f &= (1/4\pi kT) \\ (E_f/E_i)^{1/2} \exp(-\beta/2) \sigma_{es} S(\alpha, \beta) dE_f d\Omega_f, \end{aligned} \quad (2.35)$$

where

$$\begin{aligned} \alpha &\equiv (E_i + E_f - 2(E_i E_f)^{1/2}) \Omega_i \bullet \Omega_f / kT \text{ and} \\ \beta &\equiv (E_i + E_f) / kT. \end{aligned} \quad (2.36)$$

σ_{es} is the scattering cross section of the bound “moderating” nucleus (e.g., proton, deuteron, carbon). $S(\alpha, \beta)$, the *scattering law*, embodies the physics of the influence of the moderator structure on the scattering process. Various formulations of $S(\alpha, \beta)$ are tabulated as part of data files that document *all* the microscopic cross sections that are used in fission reactor design. These files can be found on the web site of the National Nuclear Data Center (currently, nndc.bnl.gov). The most widely used set is ENDF/B, the latest (2009) version is VII.0. In order, however, to produce the differential scattering cross sections (Eq. 2.35) for design calculations, material temperatures, T , must be identified and supplied with the corresponding ENDF files to NJOY [10], a system of computer programs which produce microscopic cross sections for use in various design programs (which will be discussed in the next section).

The remaining neutron reactions of interest all involve the formation of a compound nucleus, which will be in an excited state, $(X^{A+1})^*$, and will subsequently decay, yielding γ or γ 's (neutron capture), n (elastic neutron scattering), $n+\gamma$ (inelastic scattering), two n 's (an $(n,2n)$ reaction), p or α (charged particle production) or fissioning. The probabilities of these various outcomes for a given isotope, j , and incident neutron energy are characterized by the microscopic cross sections: $\sigma_c^j(E)$, $\sigma_s^j(E)$, $\sigma_{in}^j(E)$, $\sigma_{2n}^j(E)$, $\sigma_p^j(E)$, $\sigma_\alpha^j(E)$, and $\sigma_f^j(E)$. As noted above in the discussion of Q factors, for endothermic reactions, $Q < 0$, cross sections will be zero until a threshold value of E for the initiating neutron is reached. This is the case for inelastic scattering, $(n,2n)$ and some (n,α) and (n,p) reactions. There is similar threshold behavior for fertile isotope fission cross sections (see Sect. [Fission and Its Products](#)), which when the reactions “go” are exothermic. All neutron capture reactions (n,γ) are exothermic, and thus their cross sections are nonzero over the full range of fission reactor neutron energies.

One can view the “compound nucleus reaction” cross sections as the product of a cross section for compound nucleus formation, σ_C (neutron capture by the target nucleus), times the probability of a particular decay mode of the excited compound nucleus. Both factors of this “product” depend on the nature of the target and compound nuclei, X^A and X^{A+1} , and the energy available to excite the compound nucleus, X^{A+1} . The later is the sum of the reduced mass (i.e., center of mass) kinetic energy of the initiating neutron:

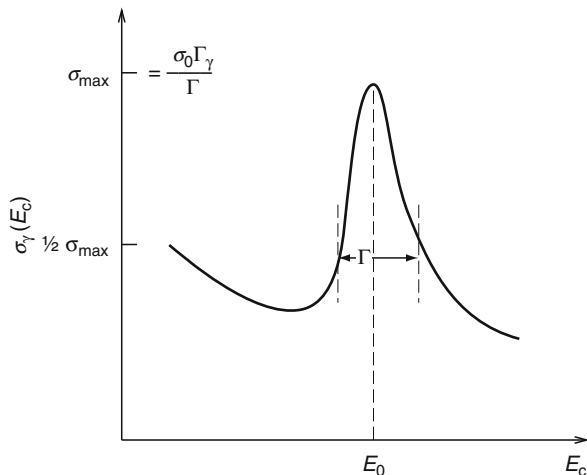
$$E_C = E(M_X/(m_n + M_X)) \cong E(A/(1 + A)), \quad (2.37)$$

where X^A is assumed to be at rest and momentum is conserved; and the excitation energy, E_e (see [Eq. 2.17](#)), provided by adding a neutron to X^A . E_e is the binding energy of the “added” neutron in the compound nucleus.

The magnitude of σ_C depends on the structure of X^A . First, if neutron number N ($=A-Z$) is odd, σ_C is larger than its counterpart for neighboring isotopes with even neutron numbers. The opposite is true for N even. This just reflects the binding energy advantage of pairing half-integral spin Fermions in a nucleus (see the discussion of B_4 in Sect. [Fission and Its Products](#)). Second, for nuclei of various A 's there are *Magic Numbers* for both Z and N (2, 8, 20, 50, 82 and 126) which can be thought of as closing shells of protons and neutrons, analogous to atomic electron shells. The reduction of σ_c for a magic number N nucleus, relative to its $N + 1$ isotope neighbor's σ_C , is much larger than the pairing effect.

Excited compound nuclei have mean lifetimes, τ (see [Eq. 2.14](#)) of as long as 10^{-14} s (Kaplan), much longer than the transit time for a neutron crossing a target nucleus, $\sim 2R/v$. Given the nuclear diameter, $2R \sim 10^{-12}$ cm, the transit time for even a *thermal* neutron is $\sim 10^{-17}$ s (The term *thermal neutron* refers to the most probable energy of the neutrons in thermal equilibrium in a zero-power reactor (e.g., a mockup). At 20°C, this is 0.023 eV, with a corresponding neutron speed of 2,200 M/s.). Thus, the standard assumption is that the decay of an excited compound nucleus is independent of all but the input energy of the initiating neutron.

Fig. 2.6 A typical neutron capture cross section for an isolated (single) resonance whose width at half maximum is Γ , the total level width. Γ_γ is the partial width for gamma ray emission from the excited state (level). E_c is the center of mass (reduced mass) energy of the initiating neutron (Duderstadt)



The decay modes of a particular excited state, nuclear level, are characterized by a *level width*

$$\Gamma \equiv h/(2\pi\tau), \quad (2.38)$$

with dimensions of energy (h is Planck's constant, 4.135667×10^{-15} eV-s), which is based on the Heisenberg uncertainty principle. In a quantum mechanical system like our excited compound nucleus, knowledge of energy and time is governed by

$$\Delta E \Delta t \sim h/2\pi. \quad (2.39)$$

Thus, Γ can be viewed as the uncertainty in energy of an excited state (level) of a compound nucleus, and τ a measure of the “uncertainty” of the lifetime of the excited state. The microscopic neutron cross sections, which go through the compound nucleus formation process, exhibit resonance behavior (peaking) when the neutron energy and E_c (the added neutron binding energy) produce or nearly produce a well-defined excited state (i.e., having a small Γ). See Fig. 2.6.

The level width Γ can be thought of as the probability per unit time of decay of an excited state and thus the sum of partial “widths” (probabilities per unit time) for each mode of decay:

$$\Gamma = \Gamma_\gamma + \Gamma_n + \Gamma_{n\gamma} + \Gamma_f + \Gamma_{2n} + \Gamma_p + \dots, \quad (2.40)$$

(where Γ_n refers to elastic compound scattering and $\Gamma_{n\gamma}$ refers to inelastic scattering, the rest being obvious).

Therefore, a “compound nucleus reaction” cross section near an isolated resonance is

$$\sigma(n, i) = \sigma_C(n) \Gamma_i / \Gamma, \text{ for } i = \gamma, n, (n\gamma), f, 2n, p, \text{ etc.} \quad (2.41)$$

The functional form of $\sigma(n, i)$, its dependence on neutron energy, was derived with the principles of quantum mechanics by Briet and Wigner [11] in 1935. Their “formula” for this simple case is

$$\sigma(n, i) = (\lambda^2/4\pi)\Gamma_n\Gamma_i / \left[(E - E_0)^2 + (\Gamma/2)^2 \right], \quad (2.42)$$

where λ is the de Broglie wavelength of the neutron, $h/(2m_n E)^{1/2}$, and E_0 is the energy of the resonance peak. Figure 2.6 is an illustration of this “form” for $i = \gamma$.

Briet and Wigner’s most impressive derivation is more general than Eq. 2.42.

First, they considered neutron energies beyond what has been found pertinent to fission reactors. When one accounts for conservation of angular momentum, the initiating neutron has classically a magnitude of angular momentum $|L|$ equal to pb , where p is neutron momentum, $(2m_n E)^{1/2}$, and b is the displacement of the neutron path from a parallel axis running through the center of the target nucleus. In a quantum mechanical treatment,

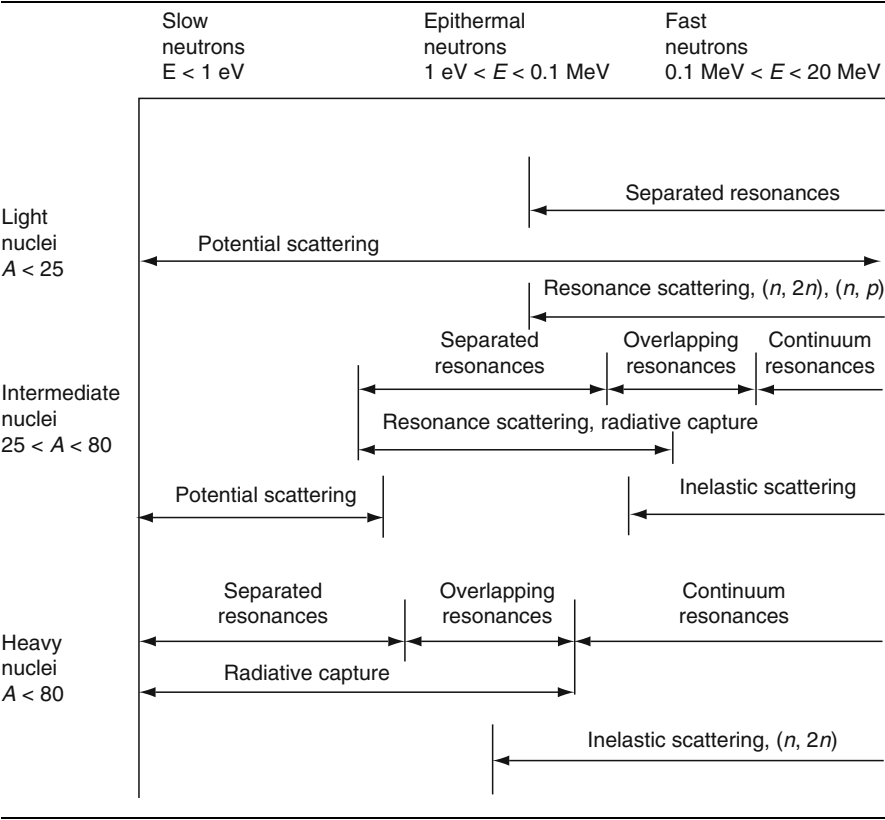
$$|L| = (l(l+1))^{1/2}h/2\pi \text{ where } l = 0, 1, 2, 3, \dots \quad (2.43)$$

Then, one can think of “ b ” as $|L|$ (given by Eq. 2.43) divided by the neutron momentum, p , and if there is going to be a significant probability of a reaction with the target nucleus, “ b ” cannot be much larger than the target nucleus radius, $r \cong A^{1/3}(1.28 \pm 0.05) \times 10^{-13}$ cm. For this to be true for a large nucleus, for example, for U^{235} , and for nonzero angular momentum (e.g., $l = 1$), the neutron would have to have kinetic energy ≥ 6.6 MeV. For smaller nuclei the required energy would be greater. Given the spectrum of neutrons in fission reactors, where most neutrons are born at around 2 MeV (see Fig. 2.4), an assumption of zero angular momentum ($l = 0$) for the vast majority of reactions is good, and thus equation Eq. 2.42 does not include a factor involving angular momentum or spin quantum numbers. This assumption also means that decay products of an excited compound nucleus will be released isotropically in the center-of-mass coordinate system, which is reflected in the factor of $1/4\pi$ in Eq. 2.42 (the probability that the decay product i ($i = n, \gamma, p$) is released $d\Omega$ about any Ω). The quantum mechanical treatment of angular momentum also accounts for the statement made above that “billiard ball” elastic scattering “can be assumed to be isotropic in the center of coordinate system.” This direct elastic scattering is referred to as *potential* scattering so as to be differentiated from resonance (compound nucleus) elastic scattering, that is, $i = n$ in equation Eq. 2.42.

Second, Breit and Wigner recognized and treated interference between potential and resonance elastic scattering. They found that the total elastic scattering cross section dips at energies right below the resonance peak, E_0 .

Finally, as they were aware that there could be multiple possible excited states of a compound nucleus they extended their “formula” to two resonances whose Γ s do not overlap.

Table 2.6 Types of neutron cross section for various target element/isotope masses pertinent to fission reactor design



Since Breit and Wigner’s original work, there has been great activity in measuring cross sections, motivated principally the desire to understand the physics of the nucleus. In the process, however, the basic parameters required for nuclear weapon and reactor design were generated. The neutron cross sections for fission reactor design are summarized in Table 2.6 [12].

In this table, the distinction is made between resonance cross sections with different densities (spacing) of resonance peaks. With intermediate and heavier nuclei the level structure grows more complex, and the number of possible excited states of a compound nucleus greatly increases. With higher neutron energy more finely spaced excited states can be reached and their level width, Γ ’s, increasingly overlap until measurement cannot resolve individual resonances.

In parallel with the work of nuclear spectroscopy experimentalists, theoreticians have built on Breit and Wigner’s work. Resonance cross-section models [13] are key to creating Evaluated Nuclear Data Files. The Cross Section Evaluation Working Group, a cooperative effort of national laboratories, industry and universities in

the United States and Canada (see nndc.bnl.gov), sponsors reviews of the various measurements of a given cross section (target isotope and reaction) and the subsequent determination (As part of the process of evaluating nuclear data sets, very accurate calculations of integral experiments are made. Zero power *mockups* of reactors, with carefully recorded dimensions and inventories, are commonly used. Monte Carlo calculations (to be discussed in the next section) of neutron balance in the mockups are made with various data sets (e.g., cross-section libraries) to determine a recommended set. See the CESWG website for references to such experiments.) of a consensus set of parameters for an appropriate cross-section *model*. These models and their “consensus” parameters are a large part of the ENDF/B-VII.0 data files. Having the cross sections represented by an analytic model also facilitates dealing with the temperature effect on resonance cross-sections. that is, Doppler shift or broadening. The analytic process of averaging a resonance cross section (i.e., its model), over the velocity distribution of the target nuclei at a given temperature is similar to what was discussed above for reactions initiated by neutrons in thermal energy range. The process is outlined by Duderstadt and Hamilton using the single-level Breit Wigner formula as the resonance model. The effect of increasing temperature is to reduce a resonance peak while broadening its width, thus increasing its Γ . To first order, the area under the resonance is unchanged, which could lead one to think that resonance “Doppler” broadening is not an important effect in a reactor application. This is true if the density of the resonance target nuclei is small (i.e., it is very dilute in the reactor), and thus its presence does not change the energy dependence of the reactor’s neutron population. However, in most reactor designs, resonance absorbers are concentrated in localized reactor features (e.g., fuel elements, control rods) and there is significant self-shielding at the resonance peak. That is, neutrons with the “peak” energy will most likely be absorbed in the reactor “feature” irrespective of temperature-induced changes in the resonance microscopic cross section. But the story can be different on the wings of a resonance where the cross section is much smaller, and, thus, so is the self-shielding. An increase in temperature of the “feature” can result in a net increase in neutron absorption, with no change at the peak energy, but with increases in the wings. This phenomena can aid in insuring a *negative temperature coefficient* for a fission reactor design (*Temperature coefficients* are collective reactor parameters that reflect how neutron balance is impacted by temperature change through feedback mechanisms, for example, Doppler broadening (or narrowing) of resonances, and moderator density changes. Reactor control will be discussed in Sect. [Fission Reactor Performance](#).). A negative temperature coefficient is a crucial reactor design safety requirement.

Dealing with temperature in producing resonance cross sections for design calculations is handled in a manner similar to the process for thermal energy range cross sections discussed above. The ENDF resonance cross-section models and appropriate material temperatures are input to NJOY, and the output are the broadened cross sections in the model format. How these cross sections are used in design calculations is addressed in the next section.

As noted at the start of this section, gamma ray (photon) cross sections are important in fission reactor design as they are required for the full treatment of energy deposition throughout a reactor (in its fuel bearing *core* and supporting structures). In the order of importance with increasing gamma energy, the mechanisms of attenuation are the photo electric effect (γ, e^-), Compton scattering (γ, γ^*), and pair production (γ, e^-e^+). The photoelectric effect removes a γ when its energy, $h\nu$, can eject an atomic electron. Its cross section is approximately proportional to $Z^4/(h\nu)^3$, and has discontinuities in energy as the ionization energy of various atomic electron shells are achieved. For higher γ energies, Compton scattering interactions with atomic electrons can be treated as effectively free electron collisions. Conserving momentum and energy relativistically, one can derive expressions for energy loss and change in direction for initiating γ s as a function of their incident energy. The magnitude of the cross section is proportional to Z . When γ energies reach a threshold of 1.022 MeV ($2 \times m_e c^2$) and are in the field of a target nucleus, pair production of an electron and positron is possible. The magnitude of the pair production cross section is proportional to Z^2 . Of course, in tracking the γ population in a reactor, one recognizes that annihilation of a positron will produce two 0.51 MeV γ 's. So pair production can be viewed as a form of inelastic scattering event. Cross sections for these three processes are tabulated in ENDF/B files, and they are described at a thorough but accessible level in the classic text by Robley D. Evans "The Atomic Nucleus."

An example plot of these cross sections for Th^{232} is provided in Fig. 2.7.

Finally, there are other gamma reactions which can take place in a reactor, for example (γ, f) and (γ, n) (the latter which we noted earlier as a source of delayed neutrons). However, these are threshold reactions for relatively high-energy gammas, and as shown in Table 2.3 the total energy available from fission from fissile isotopes for gammas is limited: <8 MeV for prompt γ 's, and, <6.5 MeV for delayed γ 's. Thus, these reactions are not important in determining the overall distribution of gammas in a reactor design.

Neutron Distributions

With the material provided to this point, the primary problem of reactor *theory* can be addressed: that of finding the neutron distribution in phase space ($\mathbf{r}, E, \boldsymbol{\Omega}$), of a reactor design, and subsequently the reactor's power distribution, both throughout the reactor design's lifetime. The first task is to derive the equation for the neutron density, $N(\mathbf{r}, E, \boldsymbol{\Omega})$, the neutron transport equation, and auxiliary equations for the atom densities, $\rho_j(\mathbf{r}, t)$, of depleting (initial inventory) isotopes and important fission products (Like reactor physics, *reactor theory* is a traditional term in the nuclear engineering discipline. It refers to the study of the neutron transport equation and the means of its solution.). A simple approach to deriving the transport equation is to consider a balance relationship for $N(\mathbf{r}, E, \boldsymbol{\Omega}, t)dE d\boldsymbol{\Omega} dt$ for a time invariant volume, V , in configuration space:

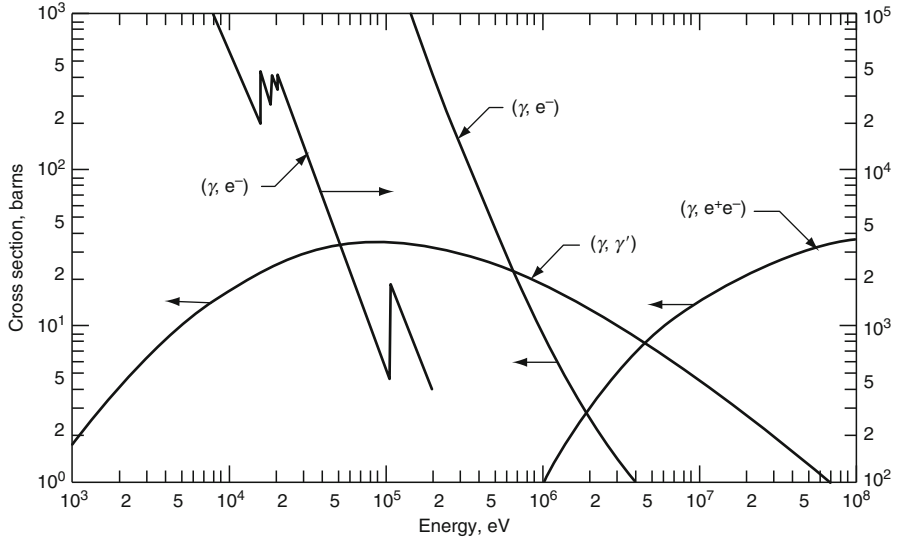


Fig. 2.7 Thorium cross section for the photo electric effect (γ, e), for Compton scattering (γ, γ'), and pair production ($\gamma, e^+ e^-$) [32]

$$\begin{aligned}
 dE d\Omega dt \int_V (\partial N(\mathbf{r}, E, \Omega, t) / \partial t) d^3 \mathbf{r} = & -\text{loss from flow out of } V \\
 & + \# \text{ scattering into } dE \text{ about } E \text{ and } d\Omega \text{ about } \Omega \\
 & + \# \text{ produced by fission} + \# \text{ produced by other sources}
 \end{aligned} \quad (2.44)$$

For the “flow” term, one defines the neutron angular current $\mathbf{J}(\mathbf{r}, E, \Omega, t) \equiv \mathbf{v}N(\mathbf{r}, E, \Omega, t)$, where $|\mathbf{J}(\mathbf{r}, E, \Omega, t) \cdot \mathbf{n}| ds dE d\Omega dt$ is the no. of neutrons at \mathbf{r} , with energies in dE about E , traveling in $d\Omega$ about Ω , which cross an area ds with a unit normal vector \mathbf{n} in dt at t . And thus, net flow out of V , which has a non-reentrant surface S , is:

$$\begin{aligned}
 dE d\Omega dt \int_S \mathbf{J}(\mathbf{r}, E, \Omega, t) \cdot \mathbf{n} ds \\
 = dE d\Omega dt \int_V \mathbf{v} \cdot \nabla N(\mathbf{r}, E, \Omega, t) d^3 \mathbf{r},
 \end{aligned} \quad (2.45)$$

where Gauss’ Theorem is applied to transform the surface integral to a volume integral.

The “reactions” in V are simply:

$$dE d\Omega dt \int_V v \Sigma_T(\mathbf{r}, E, t) N(\mathbf{r}, E, \Omega, t) d^3 \mathbf{r}, \quad (2.46)$$

where $\Sigma_T(\mathbf{r}, E, t)$ is the total *macroscopic* cross section in V . All scattering cross sections included in Σ_T have been integrated over final energies and directions.

Scattering into V is:

$$\begin{aligned} & dE d\Omega dt \int_V d^3r \int_0^\infty dE' \int d\Omega' \\ & \nu' \Sigma_s(\mathbf{r}, t, E' \rightarrow E, \Omega' \rightarrow \Omega) N(\mathbf{r}, E', \Omega', t) \end{aligned} \quad (2.47)$$

where Σ_s is the double differential *macroscopic* scattering cross section in V (see the definition Eq. 2.65 for an example of a double differential *microscopic* scattering cross section).

The direct fission source into V is:

$$\begin{aligned} & dE d\Omega dt \int_V d^3r \int_0^\infty dE' \int d\Omega'' \sum_i \nu_{pi}(E' \rightarrow E) \\ & \Sigma_{fi}(\mathbf{r}, E', t) \nu' N(\mathbf{r}, E', \Omega, t) / 4\pi, \end{aligned} \quad (2.48)$$

where $\nu_{pi}(E' \rightarrow E)$ is the number of prompt neutrons emitted in dE about E by a fission of isotope i initiated by neutrons in dE' about E' : the macroscopic fission cross section for isotope “ i ” is $\rho_i(\mathbf{r}, t) \sigma_{fi}(E')$.

The delayed neutron source into V is:

$$dE d\Omega dt \sum_j X_{dj}(E) \frac{\lambda_j}{4\pi} \int_V C_j(\mathbf{r}, t) d^3r, \quad (2.49)$$

where $X_{dj}(E)/4\pi$ is the probability that the decay of delayed neutron precursor “ j ” will produce a neutron in dE about E and $d\Omega$ about Ω , and where λ_j and C_j are, respectively, the decay constant (see the beginning of section “[Heavy Elements](#)”) and isotope density of precursor “ j ”.

And, finally any source of neutrons in V not produced by a neutron reaction is given by:

$$dE d\Omega dt \int_V d^3r S(\mathbf{r}, E, t) / 4\pi, \quad (2.50)$$

where S could characterize a source (e.g., Plutonium(238)-Beryllium(α, n) or Californium-252 (spontaneous fission)) included in a reactor design to aid in reactor start-up or S might account for decay processes yielding neutrons due to the presence of depleted fuel incorporated from another design.

Now, if the terms on the right side of the “balance relationship,” equation Eq. 2.44, are moved to the left side, and $dE d\Omega dt$ and the integral operation $\int_V d^3r$ is factored out of all the terms, then as the right side is now zero and the small volume V is arbitrary, the collection of expressions under the integral must equal zero. The resulting equation is the *Neutron Transport (or Boltzmann) Equation*:

$$\begin{aligned}
 \frac{\partial}{\partial t} N(\mathbf{r}, E, \Omega, t) = & -\mathbf{v} \cdot \nabla N(\mathbf{r}, E, \Omega, t) - \Sigma_T(\mathbf{r}, E, t) N(\mathbf{r}, E, \Omega, t) \\
 & + \int_0^\infty dE' \int d\Omega' v' \Sigma_s(\mathbf{r}, t, E' \rightarrow E, \Omega' \rightarrow \Omega) N(\mathbf{r}, E', \Omega', t) \\
 & + \int_0^\infty dE' \int d\Omega' v' \sum_i \nu_{pi}(E' \rightarrow E) \Sigma_{fi}(\mathbf{r}, E', t) N(\mathbf{r}, E', \Omega', t) / 4\pi \\
 & + \sum_j X_{dj}(E) \lambda_{dj} C_j(\mathbf{r}, t) / 4\pi + S(\mathbf{r}, E, \Omega, t). \quad (2.51)
 \end{aligned}$$

The conditions for solutions of this partial-differential-integral equation are the continuity condition:

$N(\mathbf{r} + \alpha \mathbf{\Omega}, E, \Omega, t)$ must be a continuous function of α for $\mathbf{r} + \alpha \mathbf{\Omega}$ in the reactor, and the

boundary condition:

$N(\mathbf{r}_s, E, \mathbf{\Omega}, t) = 0$, for $\mathbf{\Omega} \cdot \mathbf{n} < 0$, where \mathbf{n} is an outward unit vector normal to a non-reentrant surface chosen to define the extent of the reactor.

The auxiliary equations for number densities of delayed neutron precursors, $C_j(\mathbf{r}, t)$, and fission product poisons, depleting fissile isotopes, and *burnable* poisons, $\rho_i(\mathbf{r}, t)$ s, are simply defined as movement of these isotopes in space can be ignored. *Burnable* poisons are elements with large neutron absorption cross sections (e.g., Boron, Hafnium, Cadmium, Erbium, Gadolinium) that can be included in reactor designs to maintain neutron balance over design lifetime.

- For delayed neutron precursors:

$$\frac{\partial}{\partial t} C_i(\mathbf{r}, t) = -\lambda_i C_i(\mathbf{r}, t) + \int_0^\infty dE' \int d\Omega' \sum_j \xi_{ij} v' \Sigma_{fj}(\mathbf{r}, E', t) N(\mathbf{r}, E', \Omega', t), \quad (2.52)$$

where ξ_{ij} is the expected number of precursors of type i produced by fission of isotope j .

- For fission product poisons (e.g., Xenon-135 and its precursors Tellurium-135 and Iodine-135, and Samarium-149 and its precursors Neodimium-149 and Promethium-149):

$$\begin{aligned}
\frac{\partial}{\partial t} \rho_i(\mathbf{r}, t) = & -\lambda_i \rho_i(\mathbf{r}, t) + \lambda_{j \rightarrow i} \rho_j(\mathbf{r}, t) \\
& - \int_0^\infty dE' \int d\Omega' \rho_i(\mathbf{r}, t) \sigma_{ci}(E') v' N(\mathbf{r}, E', \Omega', t) \\
& + \int_0^\infty dE' \int d\Omega' \sum_k \gamma_{ik}(E') \sum_{fk} (\mathbf{r}, E', t) v' N(\mathbf{r}, E', \Omega', t), \quad (2.53)
\end{aligned}$$

where $\gamma_{ik}(E)$ is the expected number of poison (or poison precursor) nuclei produced by fission of isotope k induced by neutrons of energy E .

- For fissile fuel and burnable poison isotopes:

$$\frac{\partial}{\partial t} \rho_i(\mathbf{r}, t) = - \int_0^\infty dE' \int d\Omega' \rho_i(\mathbf{r}, t) \sigma_{ai}(E') v' N(\mathbf{r}, E', \Omega', t), \quad (2.54)$$

where the subscript “a” as applied to σ_a^i conventionally refers to capture plus fission for fissile isotopes. For reactor designs containing fertile isotopes, equation Eq. 2.54 will have a source term reflecting the transmutation process leading to the fissile isotope “i” (see Fig. 2.1). Additional “auxiliary” equations may be needed to deal with transmutation of one isotope of a burnable poison to another, which has a significant neutron capture cross section (for example Hafnium, which has four naturally occurring isotopes).

Solving these “auxiliary” equations, irrespective of their number, is not a calculational challenge, given one knows the neutron density, $N(\mathbf{r}, E, \Omega, t)$, as they are ordinary differential equations. Obviously, solving the neutron transport equation (Eq. 2.51) for $N(\mathbf{r}, E, \Omega, t)$ is another matter. There are several features of fission reactors, however, that make this task more tractable. First, the density of neutrons needed to produce as much power as can be removed/transferred from various reactor types to do useful work is very small, $\sim 10^7 - 10^9 \text{ \#/cm}^3$, where as the density of nuclei is many orders of magnitude larger $\sim 10^{23} \text{ \#/cm}^3$. Therefore, the neutrons can be viewed as a very dilute gas in the matrix of a reactor’s nuclei, and thus neutron–neutron collisions can be ignored (they have not been accounted for in Eq. 2.51) (Another neutron behavior that can be ignored in formulating the transport equation is the finite lifetime of a free neutron. Its mean-life is $\sim 11.5 \text{ min}$. But, as will be discussed in the next section, the lifetime of neutron in a reactor is measured in milliseconds.). Second, in the primary nuclear design calculations, where it is determined if a trial configuration, loading and geometry, of fuel, structure, moderator, coolant, control elements, and poisons, can sustain neutron balance through out the reactors lifetime objective, the time variable “t” in Eq. 2.51 can be treated in a much simplified manner. Given the initial conditions of a trial reactor configuration, it is a good assumption that the atom

densities in the various macroscopic cross sections in Eq. 2.51 can be treated as nearly constant for a significant time interval, $\Delta t \geq \text{minutes}$. With this assumption, and no neutron–neutron collisions, Eq. 2.51 is linear in $N(\mathbf{r}, E, \mathbf{\Omega}, t)$ during Δt , and solution methods for Eq. 2.51 are greatly simplified. In addition, for the interval, Δt , Eq. 2.51 can be treated as a time-independent equation. For a *primary nuclear design* calculation, one ignores the source term $S(\mathbf{r}, E, t)$ (its importance to the start-up problem will be addressed in the next section) and Eq. 2.51 becomes a linear homogeneous eigenvalue problem:

$$\begin{aligned}
 & \mathbf{v}\mathbf{\Omega} \cdot \nabla \cdot N(\mathbf{r}, E, \mathbf{\Omega}) + \nu\Sigma_T(\mathbf{r}, E)N(\mathbf{r}, E, \mathbf{\Omega}) \\
 & - \nu \int_0^\infty dE' \int d\mathbf{\Omega}' \nu' \Sigma_s(\mathbf{r}, E' \rightarrow E, \mathbf{\Omega}' \rightarrow \mathbf{\Omega}) N(\mathbf{r}, E', \mathbf{\Omega}') \\
 & = \frac{1}{k} \int_0^\infty dE' \int d\mathbf{\Omega}' \nu' \sum_j \Sigma_{fj}(\mathbf{r}, E') \\
 & \left\{ \nu_{pj}(E' \rightarrow E) + \sum_j X_{dj}(E) \xi_{ij} \right\} N(\mathbf{r}, E', \mathbf{\Omega}') / 4\pi, \tag{2.55}
 \end{aligned}$$

where $1/k$ is the eigenvalue. It has been customary to use the inverse of “ k ” as the eigenvalue and to refer to k as the multiplication factor. Note that if Eq. 2.55 is integrated over the reactor volume and E and $\mathbf{\Omega}$, then k is equal to the ratio of neutron production to neutron loss, this is the origin of its designation as a “multiplication factor.” A further simplification in Eq. 2.55 arising from the assumption of “time independence” during Δt , is that delayed neutron production can just be added to prompt neutron production. As indicated, previously delayed neutrons, though less than a percent of total neutron yield in a fission, are critical to transient reactor behavior, and, therefore, control system design, to be covered in the next section.

Before proceeding with the solution methods for Eq. 2.55, a description of how the *primary nuclear design* calculation proceeds is required for a basic understanding of reactor design, and to provide perspective on the utility of the various solution methods for the transport equation. Assuming the solution method chosen has yielded a k_i and $N_i(\mathbf{r}, E, \mathbf{\Omega})$ for the initial time interval, Δt_i where $i = 1$, then one proceeds to check design requirements, and make needed modifications to the reactor’s initial *trial configuration*. In general, this is an iterative process including other disciplines (i.e., heat transfer and fluid flow, structural analysis). If $k \neq 1$, inventories of fuel/poisons or the positioning of control elements will need to be altered to achieve neutron balance (*Control elements* (sometimes generically called control rods) are structures incorporating highly neutron absorbing isotopes. They have a dual role in fission reactor design: (1) assuring criticality (a controlled steady state chain reaction) throughout a reactor’s design lifetime, i.e., compensating for potential excess neutron production from the initial fissile loading which must

be large enough to accommodate depletion; and (2) providing safe shut down (termination of the chain reaction) of the reactor in case of an accident condition or during a planned interruption of normal operations (e.g., for plant maintenance or refueling). The same “structures” could accomplish both functions or there could be separate structures (sometimes referred to as “shim” and “shutdown” rods respectively).). The power distribution throughout the reactor must then be determined. As $N(\mathbf{r}, E, \Omega)$ is the solution to a homogeneous equation, its absolute magnitude is undetermined, but a normalization factor, p , can be established from the total thermal power rating, $P(\text{MWth})$, requirement of the design, that is from:

$$\mathbf{P} = p \int_{\text{RVol.}} d^3r \int_0^\infty dE \int d\Omega v \sum_j \epsilon_j \Sigma_{ff}(\mathbf{r}, E) N(\mathbf{r}, E, \Omega), \quad (2.56)$$

where ϵ_j is the energy release per fission of isotope j (see Table 2.3). Now given $pN(\mathbf{r}, E, \Omega)$, one can calculate the power distribution throughout the reactor

$$\mathbf{P}(\mathbf{r}) = p \int_0^\infty dE \int d\Omega v \sum_j \epsilon_j \Sigma_{ff}(\mathbf{r}, E) N(\mathbf{r}, E, \Omega), \quad (2.57)$$

and determine peak powers in fuel elements, and average and peak heat fluxes into coolant channels. Thus, fuel element and heat removal system limits can be checked. If there are violations, the *trial configuration* must be altered and new results for k and $N(\mathbf{r}, E, \Omega)$ found. From the power distribution and subsequent thermal analysis, one can also verify the temperatures that were assumed for the *trial configuration*, that is, the temperatures that were needed to define thermal scattering cross sections and Doppler broadened resonance cross sections. Finally, when all conditions are met for the first time interval, Δt_1 , where $i = 1$, the *auxiliary* equations (Eq. 2.53 and Eq. 2.54) can be solved to update inventories of fuel and poisons for the next time interval, Δt_2 . For a thermal reactor design, where the fission product poisons Samarium-149 and Xenon-135, are important, initial time intervals should be short (minutes) until equilibrium levels of these isotopes are achieved (\sim hours). Subsequent time intervals can be many hours. From this brief description of the *primary nuclear design process*, it should be clear that having accurate and efficient solution methods for the time-independent neutron transport equation is key to achieving a successful design.

There are two basic approaches to solving the time independent neutron transport equation, Eq. 2.55; the probabilistic-statistical Monte Carlo simulation method [14] where individual neutrons are traced through their life experience in a reactor, and analytic methods where the variables, \mathbf{r} , E , and (sometimes) Ω , are made discrete, thus transforming Eq. 2.55 into a matrix equation.

Monte Carlo simulation is in principle well suited for this application because the neutron density is low so the transport equation can be treated as linear. Thus,

each “experiment,” that is, neutron history, is independent of all others. Initially, a neutron is started at a randomly selected reactor location and with a randomly selected direction, Ω . Its initial energy is selected by treating a typical prompt neutron energy spectrum as a probability distribution:

$$P(E)dE = v_p(E)dE \Big/ \int_{E_{\min}}^{E_{\max}} dE v_p(E), \quad (2.58)$$

which is then “sampled” with a random number between 0 and 1. In Monte Carlo computer programs [15, 16] a sequence of random numbers is generated with an algorithm. To provide an example of “sampling,” note that in this case, given a random number n , the “sampled” starting energy E is found by simply solving the transcendental equation:

$$n = \int_{E_{\min}}^E dE' P(E') \text{ for } E. \quad (2.59)$$

Now having a speed and direction, one can “sample” (with a new random number) the probability that the neutron travels a distance x before having a collision, using equation Eq. 2.20. As this probability depends on the total macroscopic cross section, $\Sigma_T(\mathbf{r}, E)$, one must keep track of material boundaries. An initial sampling will be for the distance from the starting point of the neutron to the first material boundary it could cross. If the initial sampling results in the boundary being crossed, then there is a new Σ_T and a second sampling is performed to determine if another boundary is crossed. Eventually, either the neutron leaves the reactor or the location of the first collision is established. As the total cross section is the sum of capture, scattering, and possibly fission macroscopic cross sections for the various isotopes present, one can treat the relative magnitudes of the components of the sum as a probability distribution, which when “sampled” leads to the next step in our neutron’s history. If capture is the result, the history ends, just as it would end if the neutron leaked (escaped) from the reactor. Either capture or leakage is recorded as a “loss.” If fission is the result, the history also ends, but the number of neutrons produced (1, 2, or 3) in the fission of the “selected” isotope j , and the fission location are recorded. The number of fission neutrons is determined by “sampling” the probability distribution for fission yield of isotope j . The mean of the distribution $\bar{\nu}_j(E)$ includes delayed neutrons. The number of neutrons produced by a “history” is counted as “production.” If scattering is the result of the collision then the double differential macroscopic cross section is treated as probability distribution and “sampled” to provide a new energy and direction for the neutron. Then, the process of tracking to either escape or the next collision is repeated. Thus, the “history” proceeds until it ends as either “loss” or “production”, if “production” a starting point for a subsequent “history” and a location for energy deposition are also provided.

There are various strategies for carrying out Monte Carlo calculations and the evaluation of the statistical nature of the results. A standard approach, in outline, is to run successive groups of “histories” (thousands). Discard the first few groups, which are used to establish a reasonable fission neutron spatial source distribution, and then find the mean and standard deviations of the desired calculational results from the subsequent groups. It is most economical to get good statistics for the eigenvalue k , the multiplication factor, which is just “production” over “loss,” quantities which are accumulated over the whole reactor. Energy deposition, that is, power distribution, results are much more costly. Hundreds of groups with millions of histories per group would be required to give good statistics (a five percent 95% confidence interval) for the number of fissions in small reactor volumes (e.g., a 1 cm length of a typical PWR fuel element which has a volume of 0.7 cm^3 , out of a reactor volume of $32.8 \times 10^6 \text{ cm}^3$ (for a 3,400 MWth rating)). From this discussion, one can see why, as mentioned in section [Cross Sections](#), Monte Carlo calculations of mock-up experiments are widely used in cross-section data set evaluations, where the results of interest are changes in k , the multiplication factor. Even with the tremendous advances in computing capability which have been made to date, Monte Carlo simulation is not as yet the main line method for primary nuclear design calculations. But, as will be seen in the following description of analytic methods, it can greatly aid in improving the accuracy of the analytic methods.

When the analytic approach of making the neutron density’s variables \mathbf{r} , E and Ω discrete is applied, so as to make the computational errors in solving the transport equation comparable to an exhaustive Monte Carlo simulation, the computer resource requirements will challenge today’s largest machines (peak speeds of $\sim 2.3 \times 10^{15}$ flops (floating point operations per second) [17]).

This can be demonstrated with the large PWR used in the Monte Carlo discussion: *First*, a spatial mesh of 65.6×10^6 points would result, assuming quarter core radial symmetry, and from using a $1 \times 1 \times 2 \text{ cm}^3$ cell for averaging cross sections. (The mesh may need to be finer for highly absorbing features, e.g., fixed poisons, control elements, and can be coarser in homogeneous regions.) *Second*, the energy variable can be treated with a multigroup approximation where the energy range, $0.0 \rightarrow 10 \text{ MeV}$ is divided into intervals (groups), for example, 24 for thermal neutrons, $0.0 \rightarrow 0.625 \text{ eV}$, and 57 for the rest of the range, with most of these groups allotted to epithermal neutrons, $E = 0.625 \text{ eV} \rightarrow 0.1 \text{ MeV}$ where there is a concentration of explicit resonance cross sections (see [Table 2.6](#)). A weight function $f_g(\mathbf{r}, E)$, normalized for E to unity, is required for each interval, g . These can be calculated with infinite medium problems representing various portions of the reactor; homogeneous problems with no spatial variables, or an infinite repeating array of cells (e.g., a fuel element and surrounding coolant) with radial spatial variables, but no axial, z , dependence. The power of the multigroup approximation is that it is insensitive to the choice of weight functions and thus simplifying assumptions can be made in selecting and solving the “infinite medium” problems to generate the f_g ’s. *Finally*, the direction variable, Ω , can be dealt with through a discrete ordinate approximation [18]. The unit sphere is divided into segments, the surface areas of which sum to 4π , and

a direction vector Ω_n is assigned to each segment. The segment surface areas act as weight functions when the transport equation is integrated over a segment to yield an equation for the neutron density going in the direction Ω_n . There are various schemes for selecting ordinates and weights, the most widely known is the S_n method. All methods, however, can produce *ray effects* if “n” is too small [19]. The channeling of neutrons into a few restricted directions can produce anomalous results in reactor designs with localized neutron source regions, that is, where fissile and fertile fuel predominate in different regions (commonly referred to as seed-blanket designs). For a “highly accurate” treatment, one should let $n = 16$ in each octant, for a total of 128 ordinates. So for the “large PWR example,” the number of unknowns to be solved for in the discretized time-independent transport equation is $170 \times 10^9 (=16.4 \times 10^6$ (spatial mesh points) $\times 81$ (energy groups) $\times 128$ (ordinates)). This is clearly a formidable calculational problem. If we view the analytic approach described here as transforming Eq. 2.55 into a matrix eigenvalue equation, then the simplest solution method of matrix inversion would involve matrices of a billion by a billion. Hence, an iterative method is required [20]. Much effort in reactor *theory* has been devoted to this problem, and to simplifying the analytic approach. Iterative methods for solving matrix equations are beyond the scope of this entry, but to understand how fission reactor design is actually carried out, a description of analytic approach simplifications is needed.

The direction variable, Ω , received the earliest attention. Because the neutron population in a reactor can be viewed as a dilute gas, it was natural to assume that the variation of the neutron density in space could be approximated by $\nabla \cdot D(\mathbf{r}, E, t) \nabla vN(\mathbf{r}, E, t)$ (from Fick’s Law of diffusion). When the transport equation, Eq. 2.51, is integrated over Ω and the first term on the right-hand side is replaced by the Fick’s Law expression, the result is the time-dependent neutron diffusion equation. Equation 55 can be treated analogously to yield the time-independent neutron diffusion equation. In either case, the limitations of the diffusion approximation only become apparent in trying to define the diffusion coefficient $D(\mathbf{r}, E, t)$ (see Henry, Nuclear-Reactor Analysis). The most commonly used expression is

$$D(\mathbf{r}, E, t) \equiv 1/\{3[\Sigma_t(\mathbf{r}, E, t) - \overline{\mu_0}\Sigma_s(\mathbf{r}, E, t)]\}, \quad (2.60)$$

where $\overline{\mu_0}$ is the average of the average cosine of the scattering angle (in the laboratory coordinate system) of each isotope making up $\Sigma_s(\mathbf{r}, E, t)$. This definition (Eq. 2.60) arises from a low-order spherical harmonics expansion of $N(\mathbf{r}, E, \Omega, t)$ in the neutron transport equation. Spherical harmonics are a complete orthonormal set of special functions on the unit sphere defined by Ω (the unit vector which is at angle θ from the z axis and projects in the x–y plane at angle ϕ from the x axis);

$$Y_l^m(\Omega) = H_l^m \mathbf{P}_l^m(\mu) e^{im\phi} \text{ for } l = 0, 1, 2, 3, \dots \\ m = -l \leq m \leq l, \quad (2.61)$$

where $H_l^m = \left[\frac{(2l+1)(l-m)!}{4\pi(l+m)!dm} \right]^{1/2}$, $P_l^m(\mu) = \sin^m(\mu) \frac{d^m}{d\mu^m} P_l(\mu)$ is the associated Legendre Polynomial, $P_l(\mu) = \frac{1}{2^l l!} \frac{d^l}{d\mu^l} (\mu^2 - 1)^l$ is the Legendre Polynomial and $\mu = \cos\theta$. The spherical harmonics are normalized by the relationship:

$$\int_0^{2\pi} d\varphi \int_{-1}^1 d\mu \overline{Y_l^m(\mu, \varphi)} Y_{l'}^{m'}(\mu, \varphi) = \delta_{mm'} \delta_{ll'}, \quad (2.62)$$

where $\overline{Y_l^m}$ is the complex conjugate of Y_l^m and the Kronecker deltas, δ , are 1 for $m = m'$ and $l = l'$ and 0 otherwise.

The “low-order” spherical harmonics expansion, which yields the diffusion approximation, is for $l = 0$ and 1 (also referred to as the P1 approximation). The four functions in the expansion are:

$$\begin{aligned} Y_0^0 &= (1/4\pi)^{1/2}, Y_1^{-1} = (3/4\pi)^{1/2} \sin \theta e^{-i\varphi}, \\ Y_1^0 &= (3/4\pi)^{1/2} \mu \text{ and } Y_1^1 = -(3/4\pi)^{1/2} \sin \theta e^{-i\varphi}. \end{aligned} \quad (2.63)$$

In a Cartesian coordinate system, the expansion coefficients (for simplicity of notation the time-independent case will be treated) are $N(x, y, z, E)$, the neutron density and $N_1^{-1}(x, y, z, E)$, $N_1^1(x, y, z, E)$ and $N_1^0(x, y, z, E)$, which when multiplied by v (the speed corresponding to E) are the neutron currents in the x , y , and z directions. Before applying the P1 expansion to [Eq. 2.55](#), one needs to note that the double differential scattering cross section, $\Sigma_s(E' \rightarrow E, \Omega' \rightarrow \Omega)$ in reactor applications (where neutron polarization and Bragg scattering can be ignored) depends on $\Omega' \cdot \Omega$. Then, given the addition theorem for spherical harmonics,

$$P_l(\Omega' \cdot \Omega) = \sum_{m=-l}^l \frac{(l-m)!}{(l+m)!} P_l^m(\mu) P_l^m(\mu') e^{im(\varphi - \varphi')}, \quad (2.64)$$

$\Sigma_s(\mathbf{r}, E' \rightarrow E, \Omega' \cdot \Omega)$ can be expanded in terms of associated Legendre polynomials. This is done in two steps: first the double differential scattering cross section is expressed as an expansion in ordinary Legendre polynomials (which are a complete orthogonal set of functions)

$$\begin{aligned} \Sigma_s(\mathbf{r}, E' \rightarrow E, \Omega' \cdot \Omega) &= \Sigma_s(\mathbf{r}, E) \sum_{l=0}^{\infty} \frac{(2l+1)}{4\pi} \\ &F_l(\mathbf{r}, E' \rightarrow E) P_l(\Omega' \cdot \Omega), \end{aligned} \quad (2.65)$$

and then [Eq. 2.64](#) is substituted for $P_l(\Omega' \cdot \Omega)$. (It should be remembered that Σ_s is a macroscopic cross section, and a more complete notation would show a sum over contributions from each isotope present in d^3r about \mathbf{r} .)

Now when the P1 expansion for $N(x, y, z, E, \mu, \varphi)$ is inserted in Eq. 2.55 and the resulting equation is, in turn, multiplied by the complex conjugate of each of the four spherical harmonics functions of the P1 expansion (Eq. 2.63), and integrated over μ ($-1 \rightarrow 1$) and φ ($0 \rightarrow 2\pi$), four equations result: The first is

$$\begin{aligned}
 & \frac{\partial}{\partial x} v N_1^{-1}(x, y, z, E) + \frac{\partial}{\partial y} v N_1^1(x, y, z, E) \\
 & + \frac{\partial}{\partial z} v N_1^0(x, y, z, E) = -v \Sigma_T(x, y, z, E) N(x, y, x, E) \\
 & + \int_0^{10\text{Mev}} dE' v' \Sigma_s(x, y, z, E') F_0(E' \rightarrow E) N(x, y, z, E') \\
 & + (\text{the fission term in Eq.55 with } N(\mathbf{r}, E', \Omega') \\
 & \text{replaced with } N(x, y, z, E')).
 \end{aligned} \tag{2.66}$$

The remaining three equations are of the same form, one is provided here:

$$\begin{aligned}
 & \frac{1}{3} \mathbf{v} \frac{\partial}{\partial z} N(x, y, x, E) + v \Sigma_T(x, y, z, E) N_1^0(x, y, z, E) \\
 & = \int_0^{10\text{Mev}} dE' v \Sigma_s(x, y, z, E') F_1(E' \rightarrow E) N_1^0(x, y, z, E')
 \end{aligned} \tag{2.67}$$

With these four coupled partial-differential-integral equations, there is still considerable computational complexity. To get to the standard neutron diffusion equation, one additional approximation is made:

$$F_1(E' \rightarrow E) \cong \delta(E' - E) \mu(E'), \tag{2.68}$$

where $\mu(E')$ is the average cosine of the scattering angle in the laboratory coordinate system, and energy loss (or gain) in the non-isotropic component of scattering is ignored. Substituting Eq. 2.68 in Eq. 2.67, the relationship between N_1^0 and N is a simple partial differential equation:

$$N_1^0(x, y, z, E) = - \frac{1}{3(\Sigma_T(x, y, x, E) - \mu(E) \Sigma_s(x, y, z, E))} \frac{\partial}{\partial z} N(x, y, z, E), \tag{2.69}$$

containing the diffusion coefficient $D(\mathbf{r}, E)$ (see the definition Eq. 2.60). Given the equations of the same form as Eq. 2.69 for N_1^1 and N_1^{-1} , and substituting all three into the left-hand side of Eq. 2.66. The left-hand side becomes the standard Fick's Law expression:

$$- \nabla \bullet D(\mathbf{r}, E) \nabla N(\mathbf{r}, E) = \dots \tag{2.70}$$

As noted above, this derivation of the diffusion approximation reveals its limitations. The ability of some combination of four low-order spherical harmonic functions, Eq. 2.63, to describe the true angular distribution of the neutron density throughout a reactor will be limited to regions where the distribution is nearly isotropic, that is away from boundaries and highly absorbing features (control elements and fixed poisons). To address these limitations, special boundary conditions are used, and subsidiary calculations (to be discussed below) are made to provide “fitted” cross sections for highly absorbing features.

To make the diffusion approximation an efficient design tool, additional simplifications have been developed. The differencing of the energy variable as described above for “multigroups” can be extended to a “few group” approximation. Again, weight functions are generated using accurate solutions to small region “cell” problems, which model repeating features of a reactor. But here the weight functions are applied over much larger energy ranges, three or four to cover the energy range of 0 to 10 MeV. Furthermore, one accepts the error associated with the weight functions not perfectly representing the spatial variation of neutron density energy dependence.

The use of “cell problem” auxiliary calculations can be extended. As the core, the central fuel bearing region, of most reactor designs is made up of collections of mostly fuel elements, and possibly some fixed poison and movable control elements, assembled into modules. One can perform highly accurate (e.g., Monte Carlo or multigroup, fine spatial mesh, discrete ordinate) calculations for two-dimensional (radial) repeating arrays representations of a core’s various modules. Then, for each module type, a series of corresponding few-group diffusion approximation calculations can be carried out, in which key few group cross sections are adjusted (“fitted”) to match reaction rates from the “highly accurate” reference calculation. One can use these fitted cross sections in a full core three-dimensional few group diffusion calculation as part of the *principle design process*.

Of course, with depletion, as inventories of fuel, fission products, and poisons are updated, fitting calculations will have to be repeated. This approach is particularly suited to the design of thermal reactors, that is, PWRs and BWRs, where the proper treatment of epi-thermal and thermal neutrons, including the effects of self-shielding by fuel and poison inventories, is crucial.

In fast reactor design, where most fissions take place at energies above explicit resonances (liquid metals or gasses are coolants, and fissile and fertile densities and inventories are high (no effective moderators are present)) and the mean free path of fission neutrons is large (~ 10 cm.), the treatment of fuel, structure and coolant as an homogenized material, in formulating macroscopic cross sections, is a reasonable assumption. Treatment of the energy variable is also simpler as up-scattering is not important. As a result, multigroup, 3D discrete ordinate calculations can be used in the *principle design process* for fast reactors.

Finally, returning to thermal reactor design, there is another analytic calculational approach, which is in wide use, that should be mentioned. The general designation is Nodal Methods. There are a number of variations under this title [21], but they all have as their starting point solving 2D module array problems.

One needs to produce few group neutron distributions within each module. Each module (or depending on symmetry each half or quarter module) will be a “node.” Then coupling coefficients between nodes, both radially and axially, are generated. (It is predominately in defining coupling coefficients that the various “methods” differ.) The resulting nodal equations can be solved with modest computer resources, but, to obtain power distributions and to update inventories the full reactor neutron distribution must be constructed from the module solutions and the weights found for each node. Nodal Methods have been found to be particularly useful in applying the *primary nuclear design process* to evaluating refueling options for commercial (large scale) PWRs and BWRs, where partially depleted modules are relocated, “shuffled,” as new modules are added and fully depleted, “spent” modules removed during periodic refuelings. The computational economy of nodal methods also allows them to be applied to fully time-dependent problems, particularly for accident analyses. The nature of these problems will be discussed in the next section.

Fission Reactor Performance

In the previous section, the focus was the derivation of the neutron transport equation, and how it is solved in carrying out the *primary nuclear design process*. This quasi-static *process* involves a series of time-independent calculations of the neutron density, $N(\mathbf{r}, E, \mathbf{\Omega})$, and ultimately results in the configuration and inventories (loadings) that meet design requirements for lifetime (total energy production), and normal operation thermal performance (fuel element burn-up within limits and sufficient coolant flow provided by the design pumping power allocation). There are, however, additional design requirements that involve transients, that is, $N(\mathbf{r}, E, \mathbf{\Omega}, t)$, which will be the subject here.

The simplest approach to treating transient reactor behavior is through a “point” kinetics model. If one first multiplies the time-dependent transport equation, Eq. 2.51, by a weight function, $W(\mathbf{r}, E, \mathbf{\Omega})$, and integrates over the reactor volume, energy (the full range, $0 \rightarrow 10$ MeV), and direction ($\cos \theta$ from -1 to 1 , ϕ from 0 to 2π); and second, multiplies the time-dependent equation for each delayed neutron precursor, Eq. 2.52 for $C_i(\mathbf{r}, t)$, by $W(\mathbf{r}, E, \mathbf{\Omega})X_{di}(E)$ and performs the same integration over reactor volume, energy, and direction, the results are the point kinetics equations:

$$\frac{dT(t)}{dt} - \frac{\rho - \beta}{\Lambda} T(t) + \sum_{i=1}^I \lambda_i C_i(t) + Q(t) \quad (2.71)$$

$$\frac{dC_j(t)}{dt} = \frac{\beta_j}{\Lambda} T(t) - \lambda_j C_j(t) \text{ for } j = 1, 2, \dots, I \quad (2.72)$$

where $T(t)$ is an amplitude function;

$$T(t) \equiv \int_{\text{reactor}} dV \int_0^{10\text{Mev}} dE \int d\Omega W(\mathbf{r}, E, \Omega) N(\mathbf{r}, E, \Omega, t). \quad (2.73)$$

In formulating the expressions for the kinetics parameters, $\rho(t)$, $\beta(t)$, and $\Lambda(t)$, it is convenient to factor the neutron density into a product of “shape” and amplitude functions. The shape function is;

$$S(\mathbf{r}, E, \Omega, t) \equiv N(\mathbf{r}, E, \Omega, t)/T(t). \quad (2.74)$$

Now the weight function is defined over the same domain (space, energy, and direction) as the neutron density, and thus from the definitions [Eq. 2.73](#) and [Eq. 2.74](#) the normalization of S and W follows:

$$\int_{\text{reactor}} dV \int_0^{10\text{Mev}} dE \int d\Omega W(\mathbf{r}, E, \Omega) S(\mathbf{r}, E, \Omega, t) = 1 \text{ for all } t. \quad (2.75)$$

In order for the point kinetics equations to provide accurate solutions for small changes in reactor configuration, the weight function, $W(\mathbf{r}, E, \Omega)$, is chosen to be the solution the adjoint equation corresponding to the time-independent transport equation, [Eq. 2.55](#), for the reactor of interest adjusted to be critical (i.e., the eigenvalue $k = 1$). In the adjoint of [Eq. 2.55](#), the variable pairs (E, Ω) and (E', Ω') are interchanged in the scattering and fission terms. The solution, $N^*(\mathbf{r}, E, \Omega)$, is referred to as the adjoint neutron density or the importance function. The latter name indicates the physical interpretation of N^* . If the reactor described by [Eq. 2.55](#) is at zero power (no neutrons) and a neutron is inserted at \mathbf{r} with velocity $\mathbf{v}(E, \Omega)$, the neutron level will increase to a steady-state value (remember the reactor is still critical). This “level” per neutron added at (\mathbf{r}, E, Ω) is $N^*(\mathbf{r}, E, \Omega)$. How N^* , acting as a weight function, improves the point kinetics equations will be discussed after ρ , β , and Λ are defined and their physical interpretation given. To simplify notation, the scattering and fission integral operators in [Eq. 2.51](#) are represented by A and G :

$$A \equiv \int_0^\infty dE' \int d\Omega' v' \Sigma_s(\mathbf{r}, E' \rightarrow E, \Omega' \rightarrow \Omega), \quad (2.76)$$

$$G \equiv \int_0^{\infty} dE' \int d\Omega' v' \sum_i v_i(E') \Sigma_{fi}(\mathbf{r}, E') \bullet, \quad (2.77)$$

where $v_i(E')$ is the total number of neutrons (prompt plus delayed) produced by fission of isotope i induced by a neutron with energy E' . In reactor kinetics, delayed neutron yields are expressed in terms of the ratio the number produced with a given half-life (i.e., a member of “delayed group,” j , as noted previously, see [Table 2.4](#)) by fission of isotope, i , to the total the total yield, v_i . These ratios are represented as β_j^i , where normally $j = 1, 2 \dots 6$.

The parameter $\rho(t)$ is the *reactivity* of a reactor and is a measure of how far from criticality (a steady-state chain reaction only from fission neutrons, no other neutron sources present) the reactor is at time t . This can be seen from the expression for $\rho(t)$ that results from the derivation of [Eq. 2.71](#) from the transport equation (where the functional dependencies on \mathbf{r} , E , Ω , and t are understood for Σ_T , W , and S):

$$\rho(t) \equiv \frac{\int_{\text{reactor}} dV \int_0^{\infty} dE \int d\Omega W [- v\Omega \bullet \nabla S - v\Sigma_T S + AS + \sum_i X^i(E)GS]}{\int_{\text{reactor}} dV \int_0^{\infty} dE \int d\Omega W \sum_i X^i(E)GS}, \quad (2.78)$$

where $X^i(E)$ is the total fission spectrum for isotope i :

$$X^i(E) \equiv X_p^i(E) \{1 - \beta^i\} + \sum_{j=1}^6 X_{dj}(E) \beta_j^i. \quad (2.79)$$

Now note, if both the numerator and denominator of [Eq. 2.78](#) are multiplied by the amplitude function $T(t)$, and W is taken as 1, then the numerator is the total neutron production rate minus loss rate for the reactor. (When the first term in the bracket in the numerator is integrated, and Gauss' theorem is applied, it yields the total neutron leakage rate from the reactor.) Similarly, the denominator is the total neutron production rate. Reactivity is a dimensionless parameter whether or not W is unity. If it is zero, the reactor is critical, if negative, subcritical and if positive, supercritical.

β_j in [Eq. 2.72](#) is the *effective delayed neutron fraction* for the j th precursor group, and β in [Eq. 2.71](#) is the sum of the β_j 's:

$$\beta_j \equiv \frac{\int_{\text{reactor}} dV \int_0^{\infty} dE \int d\Omega W \sum_i X^i(E) \beta_j^i \text{GS}}{\int_{\text{reactor}} dV \int_0^{\infty} dE \int d\Omega W \sum_i X^i(E) \text{GS}}. \quad (2.80)$$

As with the expression for reactivity, multiplying the numerator and denominator of Eq. 2.80 by $T(t)$ and letting $W = 1$, one sees that in this case β_j is the fraction of total fission neutrons produced in the reactor by precursor group j .

The parameter Λ is the *prompt neutron lifetime* and is defined as:

$$\Lambda \equiv \frac{\int_{\text{reactor}} dV \int_0^{\infty} dE \int d\Omega W S}{\int_{\text{reactor}} dV \int_0^{\infty} dE \int d\Omega W \sum_i X^i(E) \text{GS}}. \quad (2.81)$$

Again multiplying the numerator and denominator by $T(t)$ and taking $W = 1$, one sees that Λ equals the number of neutrons in the reactor divided by the rate of neutron production by fission. If the reactor is critical, Eq. 2.81 has the same form as the “fundamental equation of radioactive decay,” Eq. 2.11, and Λ can be thought of as the “mean lifetime” of a neutron born into the reactor. In the point kinetics equations, Λ is the mean *prompt neutron lifetime*, and the timing of the appearance of delayed neutrons is treated explicitly through the behavior of their precursor, $C_j(t)$ $j = 1, 2, \dots, I$ (usually = 6).

The derivation of the point kinetics equations directly from the time-dependent neutron transport equation has been presented here to provide perspective on approximations that are normally made to make the generation of the point kinetics parameters (ρ , β , and Λ) practical. If Eq. 2.51 and its *auxiliary* equations could be readily solved for $N(\mathbf{r}, E, \Omega, t)$, there would be no need for the point kinetics equations. As it turns out, however, “practical” approximations follow from the approaches described in the previous section for solving the time-independent transport equation. Henry in *Nuclear-Reactor Analysis* derives the point kinetics equations starting with the diffusion approximation (with energy a continuous variable). One could just as well start with a few group diffusion approximation which would provide a shape function (a vector) and from the adjoint of the few group diffusion equation, a weight function (also a vector). The advantage of using an adjoint weight function, irrespective of the approximation to the transport equation one starts from, is in calculating reactivity, $\rho(t)$. In transients of interest in design, $\rho(t)$ is the driver. It reflects changes in cross sections with time due to variations in temperature (coolant density, Doppler effects) and configuration (control rod motion). In whatever form Eq. 2.78 takes, given the neutron transport approximation used, if a changing cross section is represented as a starting value plus a time-varying small delta, $\delta \Sigma(\mathbf{r}, E, t)$, and the shape function is represented as a time-independent function (e.g., from the initial neutron density of the reactor,

the same problem that generates the adjoint) plus a time-dependent small delta, $\delta S(\mathbf{r}, E, t)$, then the resulting calculation of $\rho(t)$ will to first order in deltas only depend on $\delta \Sigma(t)$'s. Higher order terms can be ignored, and one does not need to calculate a time-dependent shape function. This is a classic perturbation problem. Henry (chapter 7) provides a detailed derivation.

The time dependence of $\beta_j(t)$ and $\Lambda(t)$, Eq. 2.80 and Eq. 2.81, as used in the point kinetics equations can be ignored in most applications. Measured values of β (and the β_j^i from which it is summed) can be used directly (Table 2.4). If adjoint weighting is used, the β 's will be a bit larger than the physical β 's in a thermal reactor due to the increased “importance” of delayed neutrons with their lower initial energies (relative to prompt neutrons). Prompt neutron lifetimes primarily depend on the reactor type; for thermal reactors they are on the order of $\sim 10^{-3}$ s, and for fast reactors as short as 10^{-7} s. They can be measured in zero power reactor mock-up experiments as ratios with β and ρ , or calculated directly from equation Eq. 2.81 with the approximations for W and S used to obtain ρ . A highly accurate calculation of Λ can be made with a Monte Carlo simulation where neutrons are introduced from the prompt neutron energy spectrum with an $S(t = 0)$ spatial distribution. Each history would be timed and terminated with neutron absorption (capture plus fission) or leakage. The “times” will yield the mean and standard deviation of the prompt neutron lifetime.

One further note on reactivity, if a perturbation of a critical reactor configuration can be viewed as nearly instantaneous, that is, a step change, then a good estimate of reactivity addition or subtraction can be found by solving the eigenvalue (time independent) problem for the perturbed reactor:

$$\rho = 1 - 1/k, \quad (2.82)$$

and if the initial reactor configuration is subcritical then the reactivity addition from a “step” perturbation can be found by performing two eigenvalue problems, the perturbed case as before, and one for the initial subcritical configuration (ignoring any nonfission source);

$$\rho = 1/k_o - 1/k, \quad (2.83)$$

where $k_o (<1)$ is the initial subcritical eigenvalue. As reactivity is a dimensionless ratio, it is often given as a percentage or in units of β (as defined by Eq. 2.80). In the latter case, the “units” are traditionally dollars and cents. If ρ equals β , the reactivity addition is 1 dollar; if ρ equals 0.5β the reactivity addition is 50 cents. If a dollar of reactivity is added to a critical reactor, it is said to be prompt critical (critical on prompt neutrons alone) and delayed neutrons will not mitigate the resulting transient, a condition obviously to be avoided.

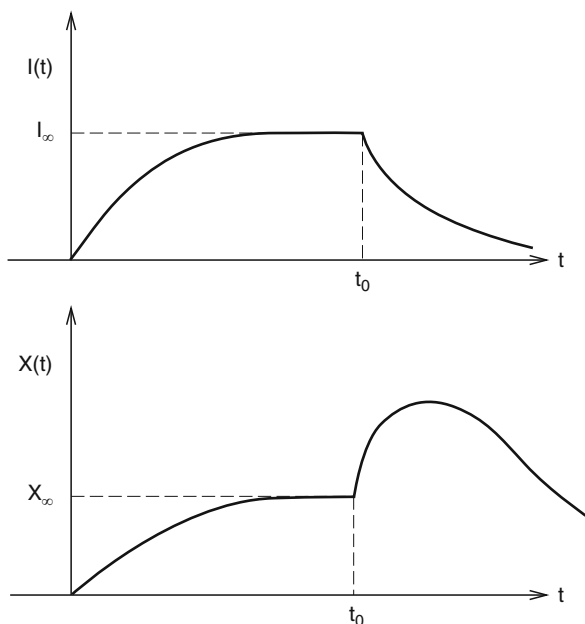
The motivation for the description of point kinetics provided here is best provided by Henry:

“Since mean free paths are fairly long and since the lifetimes of neutrons in a reactor are quite short, the effects of local perturbations on” $N(\mathbf{r}, E, \Omega, t)$ “will quickly spread throughout a reactor. The immediate consequences of perturbing a reactor locally (for example by changing a control rod slightly) is thus a readjustment of the shape of the” neutron density. In many cases this readjustment is slight and is completed in a few milliseconds; after that the readjusted shape rises or falls as a whole depending on whether the initial perturbation increases or decreases k_{eff} . For reactors in which transients proceed in this manner, merely being able to predict the change in *level* of the neutron density “is sufficient to permit a very accurate prediction of the consequences of perturbation.”

With today’s computer capabilities, solving point kinetics problems is not a great challenge, even with time-dependent reactivity reflecting feedback from power changes in the reactor. Henry and Duderstadt provide descriptions of applicable calculational methods (development of which inspired great ingenuity in the past). In any case, to quote Henry again, point kinetics solutions provide “very accurate predictions of the consequences of (reactor) perturbations.” Thus, their utility in assuring that a reactor design satisfies fundamental transient requirements. Under normal operating conditions, a reactor must be inherently stable, that is, self-limiting. Reactivity must be reduced with increased temperature; that is, with reduced coolant density, increased mean thermal neutron energy, and Doppler broadening of resonance cross sections. These phenomena are dependent on reactor type. Clearly change in thermal neutron spectra is unimportant in a fast reactor. However, if coolant density decrease results in voiding, reactivity will dramatically decrease in a thermal reactor, but in a liquid metal cooled fast reactor increased leakage must outweigh a higher energy neutron spectrum (and an increased fission to capture ratio in fuel) to assure a negative reactivity effect. Also movement of control rods must reduce reactivity when reactor shutdown is desired. Some movable poisons, power shimming control rods, could be included in a design to flatten (make more uniform) the power distribution throughout life. (Power flattening can reduce coolant pumping power requirements. As coolant flow must meet the heat removal needs of the hottest region of the reactor, minimizing excess flow to cooler regions increases overall power plant efficiency.) But, one must assure that the operating strategy for using such rods does not compromise the speed of reactor shutdown when it is required to deal with an accident condition.

Point kinetics models can also aid in assessing *Xenon override* requirements for thermal reactors. Xe^{135} with its extremely large thermal neutron capture cross section ($\sigma_c = 2.7 \times 10^6$ b at $E = 0.023$ eV, for comparison $\sigma_f^{U235} = 577$ b at 0.023 eV) is the most important fission product poison. It is produced directly from fission and by decay of its precursor I^{135} (which is a direct fission product and has short-lived precursors, $\text{Sb}^{135} \rightarrow \text{Te}^{135} \rightarrow \text{I}^{135}$). Both Xe^{135} and I^{135} have half-lives measured in hours ($T_{1/2}^{\text{Xe}} = 9.14$ h, $T_{1/2}^{\text{I}} = 6.58$ h). So, a point kinetics reactor model will show that when a reactor is started up, Xe^{135} and I^{135} build up to equilibrium levels in about 30 h. Their levels, inventories, will depend on power level, that is, neutron density, and the reactor design must have enough excess reactivity (e.g., control rods that can be withdrawn, or for a PWR, a soluble poison in the coolant whose concentration can be reduced) to

Fig. 2.8 Schematic of I^{135} and Xe^{135} inventories following an initial reactor start-up and subsequent shutdown after equilibrium levels have been reached (i.e., at t_0). (Duderstadt)



“override” the negative reactivity perturbation of neutron capture by Xe^{135} (iodine neutron capture can be ignored). In addition, when a thermal reactor is shut down, Xe^{135} builds up as loss by neutron absorption stops and decay of I^{135} continues. The Xe^{135} inventory peaks in about 10 h to approximately three times its equilibrium level and subsequently decays. It is back to its equilibrium level in ~ 40 h (see Fig. 2.8).

Clearly additional “excess reactivity” is required to deal with a post-shutdown Xenon transient. Eventually, not being able to provide (and control) this excess reactivity can limit the useful lifetime of a thermal reactor design. As a historical aside, it was John Wheeler [3] who recognized the role that Xe^{135} and I^{135} could play in the operation of a thermal reactor. He explained the initial difficulties in operating the first plutonium production reactor at the Hanford Washington site.

While point kinetics can deal with most reactor design transient requirements, there are instances where significant spatial effects must be accounted for. In the normal operation of a large thermal reactor, there is the potential for spatial oscillations of Xenon concentrations, and therefore neutron density and power. These oscillations may not affect criticality and might only be observed by the reactor instrumentation system’s ability to measure power distributions in core. The period of these oscillations would be many hours and thus limits on coolant channel performance and fuel temperature could be compromised for extended time intervals. Space-time calculations of neutron density have to be carried out to determine if a particular design has a propensity for these oscillations. If the design is not inherently stable, its instrumentation must provide detection and an operating

strategy must be devised to suppress any oscillation initiation. With modern computing capability, few group diffusion approximations to the time-dependent transport equation, Eq. 2.51 (with explicit spatial mesh or nodal methods), can deal with Xenon oscillation evaluations [22].

There are certain reactor plant accident scenarios, which also require space-time calculations. To deal with these, nodal methods, as described in section “[Neutron Distributions](#)”, have been incorporated in safety analysis programs (see for example [23]), which model a full power plant; the reactor, its neutronics, fluid mechanics and structural integrity; and the balance of the plant, instrumentation, coolant/working fluid to power conversion, and safety systems (containment, emergency coolant injection and power supply). There are two classes of accidents where space–time effects in the reactor are important. First is “rod ejection,” where a single control rod or group of control rods is rapidly withdrawn with a large reactivity addition and neutron distribution change, in no way a small perturbation in the point kinetics sense. Second is a “cold water accident” applicable to a PWR. In this case, in a plant with multiple piping “loops” carrying coolant to the reactor, if one of the loops is not functioning so that water in the loop has cooled below the normal inlet temperature of the reactor, and the loop is reactivated (its pump turned on and isolation valves (if any) opened), while the reactor is critical, there can be large asymmetric reactivity insertion, again, this is not a small perturbation problem.

Finally, there is an additional aspect of reactor neutron time variation, which has interesting *Physics*. The transport equation, derived in section “[Neutron Distributions](#)”, is for the *mean* neutron density, $N(\mathbf{r}, E, \boldsymbol{\Omega}, t)$, but clearly as neutron interactions and production, and fission product decay are inherently probabilistic, there are fluctuations in the neutron population in a reactor (and as there are in delayed neutron precursor populations). These fluctuations were recognized early on in the Manhattan Project and are also referred to as neutron noise [24]. There are several approaches to modeling of the phenomena. The most fundamental is based on the derivation of the neutron transport equation from the quantum Liouville equation (Osborn and Yip [25]). This derivation is extended to produce an equation for the neutron doublet density, $N^{NN}(\mathbf{r}, E, \boldsymbol{\Omega}, \mathbf{r}', E', \boldsymbol{\Omega}', t)$, the expected number of neutrons in d^3r about \mathbf{r} , with energies in dE about E , going in the solid angle $d\boldsymbol{\Omega}$ about $\boldsymbol{\Omega}$ times the expected number in d^3r about \mathbf{r}' , and so on for E' and $\boldsymbol{\Omega}'$, where as in the transport equation neutron–neutron collisions are ignored. Additional equations for neutron–precursor and precursor–precursor doublet densities are produced to complete the set of equations needed to solve for N^{NN} . One also needs equations for the “mean” (in Osborn’s nomenclature, singlet) neutron and precursor densities, which were derived in section “[Neutron Distributions](#)” (Eq. 2.51 and Eq. 2.52). Being able to solve for N^{NN} is, however, not sufficient to predict the results of neutron “noise” experiments in a reactor. Equations for doublet and singlet densities for events (D) in detectors (e.g., pulse or continuous currents in an ionization chamber) are also needed. With N^{DD} and N^D one can predict variance to mean ratios of counts or the power spectral density of the current in a single detector, and the cross power spectral density of currents in two detectors

[26]. These experiments are usually performed in a reactor in a steady-state condition (in the mean of course) at zero power, critical or slightly subcritical, to obtain estimates of point kinetics parameters. These experiments have the advantage of verifying expected kinetic performance without putting the reactor into a transient. They are performed at low neutron levels because as power is increased fluctuations become negligible relative to the mean. Detector noise measurements (psd and cpsd) are sometimes made at power in operating reactors to monitor for unplanned mechanical motion, or loose parts. Modeling for these measurements is deterministic.

Fluctuations in neutron populations must be considered in developing initial start-up procedures for a newly constructed reactor (In a reactor design which incorporates fuel (including fission products and transuranics) from a previously operated reactor, natural source levels will most likely be high enough to allow “fluctuations” to be ignored.). The mean neutron density before start-up depends on an external source of neutrons, $S(\mathbf{r}, E)$ (not from neutron reactions, Eq. 2.50) which, as part of the design, could be adjacent or internal to the reactor. At start-up, the reactor is subcritical ($k < 1$) and the mean neutron population, in a point reactor sense, is $N = \Lambda S(k/(1-k))$. In outline, the steps to bring the reactor critical are to pull control rods up (down in most BWR designs) from their fully inserted position so as to insert some precalculated amount of reactivity and then wait for a new steady neutron level to be achieved. The subcritical neutron level is monitored by the reactor’s source range detectors. A power reactor is instrumented with detectors for the full range of expected neutron levels. These pull-and-wait steps are repeated until the reactor is slightly super critical, and thus the neutron level is observed to be on a continuously increasing, but easily controlled, trajectory. A pull-and-wait procedure needs to account for neutron level fluctuations because if the observed level, due to a minimizing fluctuation, is below the expected (mean) level when the reactor is actually close to its critical configuration, then the next “pull” might produce an unacceptable rapidly increasing trajectory [27]. The simplest way to avert a problem with a pull-and-wait procedure is to assure that the sources provided in the design (In a reactor design which incorporates fuel (including fission products and transuranics) from a previously operated reactor, natural source levels will most likely be high enough to allow “fluctuations” to be ignored.) are strong enough to render subcritical neutron fluctuations negligible. Of course, one has to understand neutron level fluctuations to make this assessment [28].

Future Directions

Fission reactor development, since its inception, has progressed with advances in computing capability. Early on, analog computers were used for transient analyses, but digital computers have been the primary tool. Design codes have been adapted to advancing digital technology; scalar processing, then vector processing and now

massively parallel processing. This is an active field today and should continue to be so, particularly as the drivers for improve computer technology are universal. In section “[Neutron Distributions](#)” the two approaches to solving the neutron transport equation, Monte Carlo simulation and analytic methods (differencing variables and solving the resulting matrix equations) were described. Parallel computing would appear to be well suited to Monte Carlo as independent histories can be run on the various (1,000’s of) processors simultaneously. There is, of course, the need to provide the reactor configuration (geometry, nuclide inventories, and cross sections) and the Monte Carlo code itself to each processor that runs a history. This challenge is being accepted with considerable success as exemplified by the accomplishments of the Los Alamos National Laboratory group working on the MCNP code [15] and the joint effort at the Knolls and Bettis Atomic Power Laboratories on the MC21 code [29]. Advocates of the analytic approach have, however, not accepted the ultimate triumph of Monte Carlo. This is clear in the work of a group at the Argonne National Laboratory, which has modestly named their multigroup, discrete ordinate code UNIC, for Ultimate Neutronic Investigation Code [30]. They are demonstrating impressive results for fast reactor designs. Competition in supercomputer development and in attendant codes for nuclear reactor design bodes well for better products in the future.

Physicists in their efforts to understand the atomic nucleus have made myriad measurements and only partially by design these have included the neutron and gamma cross sections, and fission product yields (and their decay mechanisms) needed for the development of fission reactors. Today, work on this reactor-related data is focused on establishing well-founded uncertainty measures. The Cross Section Evaluation Working Group of the National Nuclear Data Center refers to this effort as covariance evaluation [31]. This is particularly appropriate, for as discussed above, one expects calculational methods to improve with computer power and code development. Thus, in assigning error bounds in design, the uncertainty in basic data will become more important relative to the contribution of calculational error (e.g., Monte Carlo statistics or differencing and convergence error in analytic methods). More well-founded and hopefully smaller design error bounds can obviously be taken advantage of in future reactor development. Improving error bounds is also consistent with the approach to overall power plant safety analysis being fostered by many of the world’s nuclear regulatory agencies. They favor best estimate analyses plus the assignment of rigorously defined uncertainty factors for various classes of accident conditions. Reactor design error is only a contributor to a safety analysis “uncertainty factor,” but for power plant technology to advance, “reactor design” must do its part.

Much of the research for a next generation of fission reactor power plants is focused on higher operating temperatures. Today’s thermal reactor plants, PWRs, BWRs, and CANDU (heavy water moderated) have outlet reactor coolant temperatures, T_H , of $\sim 600^\circ\text{F}$, and thus thermal (Rankine cycle) efficiencies in the low 30%. Raising T_H would increase cycle efficiency and lower fuel cost, and provide high-temperature process heat (possibly for a catalytic hydrogen production process). Higher operating temperatures in a water (or heavy water)

environment present core and structural materials challenges. There likely will be a need for additional resonance cross-section data for some additives (e.g., Manganese and Chrome) to new high-temperature materials. Fast reactors (liquid metal or gas cooled) operate at much higher temperatures than thermal reactors but also require much higher fissile inventories to attain criticality. Experience with design and operation of these reactors is limited (especially for gas cooled reactors) compared to thermal reactors. Their future development with emphasis on the burning of unwanted transuranics as well their traditional mission of efficient conversion of fertile isotopes (U^{238} and Th^{232}) to fissile isotopes (Pu^{239} , Pu^{241} and U^{233}) will stimulate some cross-section work. But, both thermal and fast reactor development will most likely benefit more from advances in branches of physics other than Nuclear, particularly Condensed Matter and Fluid Mechanics. The need for nuclear power, both economic and environmental (if they can be separated?), will drive fission reactor development. While Uranium and Thorium are abundant in the earth's crust, power demand will push reactor development to most efficiently exploit the highest grade ores, which will likely lead to a mix of fast and thermal reactors. In any case, physics as well as engineering will play key roles in this development.

Bibliography

Primary Literature

1. Wheeler JA (1967) Mechanism of fission. *Phys Today* 20(11):49–52
2. Bohr N, Wheeler JA (1939) The mechanism of nuclear fission. *Phys Rev* 56:426
3. Ford KW (2009) Wheeler's work on particles, nuclei, and weapons. *Phys Today* 62(4):29
4. Fermi E, Szilard L (1955) Neutronic reactor. US Patent 2,708,656, 17 May 1955
5. Einstein A (1905) On the electrodynamics of moving bodies. *Ann Phys* 17:891–921
6. Frankel S, Metropolis N (1947) Calculations in the liquid-drop model of fission. *Phys Rev* 72:914
7. Kinsey R (1979) Compiler "ENDF/B Summary Doc." BNL-NCS-17541(ENDF-201), 3rd edn. ENDF/B-V, Brookhaven National Laboratory, Upton
8. England TR, Wilson WB, Stamatelatos MG (1976) Fission product data for thermal reactors. EPRI-NP-356, Los Alamos Scientific Lab., New Mexico
9. Parks DE, Nelkin MS, Wikner NF, Beyster JR (1970) Slow neutron scattering and thermalization with reactor applications. Benjamin, New York
10. MacFarlane RE (1994) The NJOY nuclear data processing system, Version 91, report #LA-12740-M, Los Alamos National Laboratory, New Mexico
11. Breit G, Wigner E (1936) Capture of slow neutrons. *Phys Rev* 49:519
12. Beckurts KH, Wirtz K (1964) Neutron physics. Springer, Berlin
13. Larson NM (2006) Updated user's guide for SAMMY: multilevel R-matrix fits to neutron data using Bayes' equations, ORNL/TM-9179/R7. Oak Ridge National Lab, OakRidge
14. Spanier J, Gelbard EM (1969, 2008) Monte carlo principles and neutron transport problems, Dover, New York, Addison-Wesley, Reading

15. X-5 Monte Carlo Team (2003) MCNP – A general Monte Carlo N-Particle transport code, Version 5, LA-UR-03-1987, Los Alamos National Laboratory, New Mexico
16. Onds LA II, Tyburski LJ, Moskowitz BS (2000) RCP01 – a Monte Carlo program for solving neutron and photon transport problems in three dimensional geometry with detailed energy description and depletion capability, B-TM-1638. Bettis Atomic Power Laboratory, West Mifflin
17. TOP 500 Super Computing Sites, www.Top500.org
18. Lathrop KA (1972) Discrete-ordinates methods for the numerical solution of the transport equation. *Reactor Technol* 15:107
19. Lathrop KA (1971) Remedies for ray effects. *Nucl Sci Eng* 45(3):355–68
20. Varga RS (2000) Matrix iterative analysis, 2 Revised and Expandedth edn. Springer, Heidelberg
21. Henry A, Dias A, Frances W, Parlos A, Tanker E, Tanker Z (1986) Continued development of nodal methods for nuclear reactor analysis, MIT EL 86-002. Massachusetts Institute of Technology, Cambridge
22. Buslik AJ, Weinreich WA (1967) Variational calculation of complex natural modes of xenon oscillation, WAPD –TM-673 (LWB-LSBR Development Program). Bettis Atomic Power Laboratory, West Mifflin
23. Idaho National Laboratory (2009) RELAP5-D, www.INL.gov
24. Thie JA (1963) Reactor noise (an AEC monograph). Rowman and Littlefield, New York
25. Osborn RK, Yip S (1966) Foundations of neutron transport theory, Monograph series on nuclear technology. Gordon and Breach, New York
26. Natelson M, Osborn RK, Shure S (1966) Space and energy effects in reactor fluctuation experiments. *J Nucl Energy Parts A/B* 20(7):557–585
27. Hurwitz H Jr, MacMillan DB, Smith JH, Storm ML (1963) Kinetics of low source reactor startups, part I and II. *Nucl Sci Eng* 15:166
28. Clark WG, Harris DR, Natelson M, Walter JF (1968) Variances and covariances of neutron and precursor populations in time-varying reactors. *Nucl Sci Eng* 31:440–457
29. Sutton TM et al, Knolls Atomic Power Lab., Griesheimer DP et al, Bettis Atomic Power Lab. (2007) The MC21 Monte Carlo Code, LM-06K144, Proceedings (on CD-ROM) of the joint international topical meeting on M&C and supercomputing applications, Monterey
30. Palmiotti G et al, Argonne National Lab. (April 2007) UNIC Ultimate Neutronic Investigation Code, Proceeding (on CD-ROM) of the joint international topical meeting on M&C and supercomputing applications, Monterey
31. Herman M et al (2008) Covariance evaluation methodology for neutron cross sections, BNL-81525-2008. Brookhaven National Lab, Upton
32. Belle J, Berman RM (eds) (1984) Chapter 2, Natelson M, Nuclear properties of the thorium fuel cycle. In: Thorium dioxide: properties and nuclear applications, Naval Reactors Office, U. S. Department of Energy, Govt. Printing Office, Washington, DC
33. Katcoff S (1958) Fission–Product yields from U, Th and Pu. *Nucleonics* 16(4):78

Books and Reviews

Duderstadt JJ, Hamilton LJ (1976) *Nuclear reactor analysis*. Wiley, New York

Evans RD (1955) *The atomic nucleus*. McGraw-Hill, New York

Henry AF (1975) *Nuclear-reactor analysis*. MIT Press, Cambridge

Kaplan I (1962) *Nuclear physics*, 2nd edn. Addison-Wesley, Reading

Krane KS (1988) *Introductory nuclear physics*. Wiley, New York

Mermin ND (2005) *It's about time, understanding Einstein's relativity*. Princeton University Press, Princeton

Nuclear Energy

Selected Entries from the Encyclopedia of Sustainability

Science and Technology

Tsoufanidis, N. (Ed.)

2013, VI, 530 p.,

ISBN: 978-1-4614-5716-9